Neuronal Detection Triggers Systemic Digestive Shutdown in Response to Adverse Food Sources

Yating Liu[#], Guojing Tian[#], Ziyi Wang, Junkang Zheng, Huimin Liu, Sucheng Zhu, Zhao Shan*, Bin Qi*

Southwest United Graduate School, Yunnan Key Laboratory of Cell Metabolism and Diseases, State Key Laboratory of Conservation and Utilization of Bio-resources in Yunnan Center for Life Sciences, School of Life Sciences, Yunnan University, China

#These authors contributed equally: Yating Liu[#], Guojing Tian[#]

* Corresponding Author：Zhao Shan (shanzhaolab@163.com) , Bin Qi (qb@yun.edu.cn)

Lead Contact: Bin Qi, Email: qb@ynu.edu.cn

Abstract

The ability to sense and adapt to adverse food conditions is essential for survival across species, but the detailed mechanisms of neuron-digestive crosstalk in food sensing and adaptation remain poorly understood. This study identifies a novel mechanism by which animals detect unfavorable food sources through neurons and initiate a systemic response to shut down digestion, thus safeguarding against potential harm. Specifically, we demonstrate that NSY-1, expressed in AWC neurons, detects *Staphylococcus saprophyticus* (SS) as an unfavorable food source, prompting the animal to avoid and halt digestion of SS. Upon detection, the animals activate the AWC^{OFF} neural circuit, leading to a systemic digestive shutdown, which is mediated by NSY-1-dependent STR-130. Additionally, NSY-1 mutation triggers the production of insulin peptides, including INS-23, which interact with the DAF-2 receptor to modulate SS digestion and affects the expression of intestinal BCF-1. These findings uncover a crucial survival strategy through neuron-digestive crosstalk, where the NSY-1 pathway in AWC neurons orchestrates food evaluation and initiates digestive shutdown to adapt effectively to harmful food sources.

Key words: Digestion, AWC neuron, NSY-1, Food behavior, *C. elegans*

Introduction

Food is a source of essential nutrients and also poses a risk of lethal toxins and pathogens. Animals, including humans, must respond to various food sources to ensure survival. The ability to detect and adapt to adverse food conditions is crucial for the survival of many species. Various sensory mechanisms have evolved to monitor food quality by detecting beneficial and harmful substances, include olfactory (Fiala, 2007; McLachlan et al., 2022; Sengupta et al., 1996), gustatory (Avery et al., 2021; Hukema et al., 2006; Scott, 2018), and gut chemosensory systems (Bargmann, 2006). Food allergies serve as a biological food quality control system, offering protection and benefits by promoting food avoidance behavior (Florsheim et al., 2021). Research by Plum et al. (Plum et al., 2023) and Florsheim et al. (Florsheim et al., 2023) provides evidence that the immune system's allergic response communicates with the brain in mice, leading to food avoidance. This avoidance behavior acts as a defense strategy, reducing the risk of exposure to harmful substances, including allergens.

The digestive system functions by transporting food through the gastrointestinal (GI) tract, where it is broken down into molecules that can be absorbed and utilized by the body's cells. Thus, shutdown of digestion may serve as a mechanism for eliminating indigestible or harmful substances, acting as a protective system in animals to avoid adverse food. Despite this, the interaction between neuronal food detection and intestinal digestion, particularly in assessing and adapting to harmful food, remains inadequately understood.

The free-living nematode *Caenorhabditis elegans* thrives in organic-rich environments where it encounters a variety of microorganisms as food (Felix and Braendle, 2010; Samuel et al., 2016; Schulenburg and Felix, 2017). *C. elegans* has evolved mechanisms to sense bacterial presence and food quality, which influence its feeding behaviors and digestive processes to adapt to its environment. Previous research has identified heat-killed *E. coli* as low-quality food, which the nematode avoids using its food-quality evaluation systems, such as the FAD-ATP-TORC1-ELT-2 pathway (Qi et al., 2017) and the UPR^{ER}–immunity pathway (Liu et al., 2024). Additionally, we have found that certain bacteria, like *Staphylococcus saprophyticus* (SS), are classified as inedible, leading to shutting down digestion and stunted growth in the nematodes (Geng et al., 2022). However,

we still need to determine whether SS represents harmful food for *C. elegans* and how the nematode senses SS and shuts down digestion to reject it. It is hypothesized that *C. elegans* may detect or assess inedible food, such as SS, and subsequently halt digestion as a survival strategy. This suggests that the cooperation between food sensing and digestive systems could form a systemic food quality control mechanism in animals, aimed at minimizing the adverse effects of harmful food.

In this study, we developed a model in *C. elegans* to investigate responses to harmful food and explored how the nematodes sense and avoid ingesting such food by shutting down their digestive systems. We identified a food quality control mechanism involving communication between neurons and the digestive system. This mechanism functions as a defense strategy to minimize the adverse effects of harmful food environments on the animals.

Results

Shutting Down Digestion as a Protective Mechanism for Survival in Larval *C. elegans*

Previous studies have shown that *Caenorhabditis elegans* cannot digest *Staphylococcus saprophyticus* (SS), which prevents their development (Figure 1A). In natural environments, *C. elegans* rely on various bacteria for nutrition and growth. However, SS is not a viable food source for *C. elegans*. Larval arrest, such as the dauer stage, serves as an adaptive mechanism for survival under unfavorable conditions, including limited food availability or extreme temperatures [8, 9]. We hypothesize that *C. elegans* can sense or evaluate inedible food, such as SS, and subsequently shut down their digestion to arrest development as a protective survival strategy (Figure 1B).

Our previous research demonstrated that *C. elegans* can assess and avoid low-quality food, like heat-killed *E. coli*, to adapt to nutrient-deficient conditions (Liu et al., 2024; Qi et al., 2017). To determine if *C. elegans* also detect SS as an unfavorable food source, we conducted two behavioral assays: food dwelling/avoidance and food choice (Qi et al., 2017). In the food dwelling/avoidance assay, larval-stage animals exhibited strong discrimination against SS compared to the standard food, OP50

(Figure 1C). In the food choice assay, the animals preferred OP50 over low-quality food such as heat-killed *E. coli* (Figure 1—figure supplement 1A) or SS (Figure 1D). However, they could not distinguish between heat-killed *E. coli* and SS (Figure 1—figure supplement 1B). These results suggest that SS acts as an unfavorable food that *C. elegans* can detect and avoid.

In response to starvation, L1 larvae can enter a state of developmental arrest, pausing their growth to survive (Baugh and Sternberg, 2006). To test whether *C. elegans* shut down digestion of SS as a protective strategy upon sensing unfavorable food, we performed a survival assay on L1 larvae fed with SS. We found that larvae unable to digest SS still survived under SS feeding conditions (Figure 1—figure supplement 1C), similar to larvae under L1 starvation. This suggests that shutting down digestion may be a protective mechanism in larvae under SS feeding conditions.

Previously, we observed that activating larval digestion with heat-killed *E. coli* or *E. coli* cell wall peptidoglycan (PGN) enabled the digestion of SS as food (Hao et al., 2024). Additionally, when animals reached the L2 stage by feeding normal OP50 diet, they could utilize SS as a food source to support growth (Figure 1—figure supplement 1D). These findings suggest that once digestion is activated (via *E. coli* components or L2-stage maturation), worms gain the capacity to process SS as a viable food source, abolishing SS-induced growth impairment (Hao et al., 2024) (Figure 1—figure supplement 1D).

If SS is indeed an unfavorable or toxic food for *C. elegans*, digesting it could result in physiological defects. We measured the lifespan of L4 stage animals fed with SS or OP50. We found that SS consumption shortened their lifespan (Figure 1E-F), indicating a cost associated with digesting unfavorable or toxic food.

In conclusion, our data suggest that larval-stage *C. elegans* can sense and evaluate SS as an unfavorable food source, leading to the shutdown of digestion to avoid consumption, thereby protecting them and allowing adaptation to an unfavorable food environment.

C. elegans **Sense SS and Shut Down Digestion through NSY-1**

We speculated that key factors in *C. elegans* are involved in sensing *Staphylococcus saprophyticus* (SS) and shutting down its digestion. If these factors are mutated, the

129 animals would fail to detect SS as an unfavorable food source and would utilize it
130 (Figure 2—figure supplement 1A). To identify these factors, we conducted an
131 unbiased forward genetic screen to find mutant animals that cannot sense SS, thereby
132 allowing its digestion and supporting growth. One of the mutant alleles identified, *ylf6*,
133 could digest SS and exhibited a growth phenotype under SS feeding conditions
134 (Figure 2—figure supplement 1B). Whole-genome deep sequencing revealed that *ylf6*
135 carries two mutations in the *nsy-1* gene (H929Y, Q1191 [stop codon*]) (Figure 2—figure
136 supplement 1C).

137 To confirm that *nsy-1* is essential for shutting down SS digestion, we used an
138 independent *nsy-1* mutant allele, *ag3*, and found that *nsy-1(ag3)* mutants also digested
139 SS (Figure 2A). To determine whether *nsy-1* is crucial for sensing SS, we performed
140 two behavioral assays: food dwelling/avoidance and food choice. In the food
141 dwelling/avoidance assay, larval stage *nsy-1* mutant exhibited significantly impaired
142 avoidance responses at both 4h and 6h but not at 8h, suggesting that NSY-1 is
143 essential for sustained aversion to SS food in the early response (Figure 2B). In
144 contrast to wild-type N2 animals, *nsy-1* mutants preferred SS when given a choice
145 between two poor-quality foods, heat-killed *E. coli* and SS (Figure 2C, Figure
146 1—figure supplement 1B). These results suggest that *nsy-1* is essential for *C. elegans*
147 to sense and avoid SS.

148 Next, we examined whether larvae that cannot sense SS and do not shut down
149 digestion can adapt to SS environments. We measured the survival rate of *nsy-1*
150 mutants under SS feeding conditions and found that these mutants had a higher
151 mortality rate (Figure 2D).

152 Overall, these results indicate that *C. elegans* sense and detect unfavorable food, such
153 as SS, through *nsy-1*, and subsequently shut down digestion to protect themselves and
154 enhance survival.

155

156 **NSY-1 Functions in AWC Neurons to Shut Down SS Digestion**

157 The *nsy-1* gene in *C. elegans* encodes a MAP kinase kinase kinase (MAPKKK) that
158 operates in the AWC neurons (Kim et al., 2002; Sagasti et al., 2001), which are
159 essential for chemotaxis and odor sensation. The primary role of *nsy-1* in AWC
160 neurons is to regulate the asymmetric expression of odorant receptors, contributing to

161 neuronal asymmetry and diversity (Chuang et al., 2007; Sagasti et al., 2001). We
162 hypothesized that the shutdown of SS digestion in *C. elegans* is mediated by *nsy-1*
163 function in AWC neurons.

164 Firstly, we constructed a P*nsy-1*::GFP reporter strain and confirmed that *nsy-1* is
165 expressed in the AWC neurons (Figure 3A). Secondly, we expressed *nsy-1* in the
166 AWC neurons of *nsy-1* mutant animals and observed that the transgenic animals
167 rescued the indigestion phenotype (Figure 3B). This indicates that *nsy-1* functions in
168 AWC neurons to shut down SS digestion. Thirdly, we used CRISPR to construct a
169 mutant strain that knocks out *nsy-1* specifically in AWC neurons (Figure 3—figure
170 supplement 1). We found that *nsy-1* knockout in AWC neurons also resulted in the
171 shutdown of SS digestion (Figure 3C). These results collectively suggest that NSY-1
172 is functional in AWC neurons and is crucial for shutting down SS digestion in *C.*
173 *elegans*.

174 Beyond its established role in AWC neurons, we detected NSY-1 expression in the
175 intestine (Figure 3-figure supplement 2A). To assess intestinal NSY-1 function, we
176 performed tissue-specific rescue experiments in *nsy-1* mutants using the
177 intestinal-specific *vha-6* promoter. Intestinal expression of NSY-1 significantly
178 suppressed the enhanced SS digestion phenotype in *nsy-1* mutants (Figure 3-figure
179 supplement 2B), demonstrating functional involvement of gut-localized NSY-1 in
180 regulating digestive responses. We propose intestinal NSY-1 mediates this effect
181 through innate immune signaling, consistent with its known pathway components. As
182 our previously established (Geng et al., 2022), the canonical PMK-1/p38 MAPK
183 pathway functions downstream of NSY-1, with both *sek-1* and *pmk-1* knockdown
184 enhancing SS digestion through immune modulation. This indicates intestinal NSY-1
185 suppresses digestion may act through PMK-1-mediated immune responses. Since
186 neuronal NSY-1's role in digestive control was previously undefined, we prioritized
187 mechanistic analysis of its neuronal function in digestion regulation.

188 To determine whether NSY-1 in AWC neurons mediates SS sensory perception, we
189 performed dwelling (avoidance) and food-choice assays using AWC-specific *nsy-1*
190 knockout and AWC-rescued strains (*nsy-1(ag3);* P*odr-1::nsy-1*). In dwelling assays,
191 AWC-specific *nsy-1* KO mutants exhibited significantly impaired SS avoidance at 6h
192 (Figure 3-figure supplement 3A), while AWC-rescued strains restored avoidance
193 capacity at 2-6h (Figure 3-figure supplement 3B). Food-choice assays further revealed

194 that AWC *nsy-1* KO mutants preferentially migrated toward SS (Figure 3-figure
195 supplement 3C), whereas AWC-rescued showed no preference between SS and HK-*E.*
196 *coli* (Figure 3-figure supplement 3D). These data conclusively demonstrate that
197 NSY-1 acts in AWC neurons to mediate SS recognition and aversion behaviors.
198

199 **AWC Neurons Exhibit OFF State in Sensing SS Food**

200 In *C. elegans*, the expression of the *str-2* gene in AWC neurons indicates the ON state
201 (AWC^{ON}) (Sagasti et al., 2001), which is associated with high cGMP levels and lower
202 calcium activity, enabling the neuron to respond to specific odors. Conversely, the
203 absence of *str-2* expression marks the OFF state (AWC^{OFF}), characterized by different
204 odor responses, low cGMP levels, and higher calcium activity (Troemel et al., 1999).
205 We aimed to investigate (1) whether AWC neurons exhibit different states under
206 normal food (*E. coli* OP50) versus unfavorable food (SS) conditions and (2) whether
207 the state of AWC neurons affects the ability of *C. elegans* to digest SS.

208 Using *str-2*::GFP as a marker for AWC neuron states (Troemel et al., 1999), we found
209 that wild-type animals feeding on normal OP50 food typically exhibit one AWC^{OFF}
210 and one AWC^{ON} neuron. However, when feeding on SS, the proportion of animals
211 with the AWC^{OFF} state increased, with approximately 50% of animals exhibiting two
212 AWC^{OFF} neurons (Figure 3D, E, F).

213 In *nsy-1* mutant animals feeding on OP50, *str-2*::GFP is expressed in both AWC
214 neurons ($2AWC^{ON}$), consistent with previous studies (Chuang and Bargmann, 2005;
215 Chuang et al., 2007; Sagasti et al., 2001; Troemel et al., 1999) (Figure 3D, E).
216 Notably, both AWC neurons remained in the AWC^{ON} state in *nsy-1* mutants feeding
217 on SS (Figure 3D, E). These results suggest that SS feeding induces an AWC^{OFF} state
218 in wild-type animals, while the *nsy-1* mutation promotes an AWC^{ON} state even under
219 SS feeding conditions. This implies that the AWC^{OFF} state may inhibit SS digestion,
220 whereas the AWC^{ON} state promotes it.

221 The TIR-1-NSY-1-SEK-1-MAPK pathway plays a crucial role in regulating the
222 asymmetric AWC cell fate decision. Previous studies have shown that *str-2*::GFP
223 expression in both AWC cells ($2AWC^{ON}$ phenotype) occurs in *tir-1*, *nsy-1*, and *sek-1*
224 mutant animals (Chuang and Bargmann, 2005; Sagasti et al., 2001; Troemel et al.,
225 1999). We found that *tir-1* mutant can grow under SS feeding conditions (Figure 3G),

226 indicating that *tir-1* mutant can digest SS similarly to *nsy-1* mutants. This
227 demonstrates that the AWC^{ON} state promotes SS digestion.

228 To confirm the important of AWC state in SS digestion, we performed AWC-specific
229 neuron ablation experiments using previously validated transgenic strain that
230 expresses cleaved caspase under the AWC-specific promoter, *ceh-36*
231 (*ceh-36p*::caspase). Critically, worms with ablated AWC neurons completely failed to
232 digest SS food (Figure 3—figure supplement 4), phenocopying the non-digesting state
233 of wild-type worms on SS. This result directly confirms that functional AWC neurons
234 are essential for initiating SS digestion, aligning with our model where the AWC-OFF
235 state (induced by SS) inhibits digestion while the AWC-ON state promotes it.

236 Overall, our data suggest that the state of AWC neurons is critical for sensing food in
237 *C. elegans*. When sensing SS food, animals exhibit an AWC^{OFF} state, which shuts
238 down digestion. Conversely, the AWC^{ON} state promotes the digestion of SS.

239

240 **NSY-1 Shuts Down SS Digestion through Induction of STR-130**

241 We have demonstrated that NSY-1 in AWC neurons detects unfavorable food and
242 shuts down digestion (Figure 3). To investigate the genes regulated by NSY-1 in
243 response to SS and their impact on SS digestion, we conducted a transcriptomic
244 analysis on L1 larval animals fed with normal food (OP50) or unfavorable food (SS)
245 for a short duration (4 hours). We speculated that some genes induced by SS food are
246 dependent on NSY-1 (Figure 4A), and their induction aids in shutting down SS
247 digestion.

248 RNA-seq data analysis revealed 304 NSY-1-dependent candidate genes responding to
249 SS (Figure 4B, Supplementary file 1). Enrichment analysis (Figure 4—figure
250 supplement 1A, Supplementary file 2) of these candidate genes showed mainly
251 associations with biotic stimulus, defense responses, xenobiotic stimulus, suggesting
252 that NSY-1 positively regulates stress response pathways to protect animals under
253 harmful food, SS, feeding conditions. Moreover, we found that sensory perception
254 related genes (*sra-32, str-87, str-112, str-130, str-160, str-230*) (Figure 4—figure
255 supplement 1A, Supplementary file 2) were also enriched, with many genes being G
256 protein-coupled receptors (GPCRs), which mediate odor sensing (Buck and Axel,
257 1991).

258 We further analyzed the dependence of these enriched GPCRs on NSY-1 under SS
259 feeding conditions (Figure 4—figure supplement 1B) and found that *str-130* is
260 significantly upregulated in response to SS, with its function strong being NSY-1
261 dependent (Figure 4C).

262 Using RNAi knockdown and the SS growth assay, we observed that RNAi of *str-130*,
263 *str-230*, *str-87*, or *str-112* significantly enhanced SS growth (Figure 4—figure
264 supplement 2A), with *str-130* RNAi exhibiting the most robust
265 phenotype—phenocopying *nsy-1(ag3)* mutants. Crucially, none of these GPCR
266 knockdowns further enhanced growth in *nsy-1(ag3)* mutants (Figure 4—figure
267 supplement 2B), confirming their position downstream of NSY-1. These data
268 establish *str-130* as the dominant effector of NSY-1-mediated SS response regulation,
269 while suggesting minor contributions from other GPCRs (*str-230, str-87, str-112*).

270 It has been shown that *str-130* is expressed in AWC^{OFF} neurons, based on transgenic
271 GFP reporter strains, *str-130p*::GFP (Vidal et al., 2018). Our data also show that
272 *str-130* expression is induced in wild-type animals fed with SS (Figure 4C), where
273 AWC neurons exhibit the AWC^{OFF} state (Figure 3D, E). Therefore, it is possible that
274 the high expression of *str-130*, regulated by *nsy-1*, alters the AWC state and inhibits
275 SS digestion.

276 Firstly, we found that knockdown of *str-130* in wild-type animals promoted SS
277 digestion, thereby supporting animal growth (Figure 4D), and the proportion of
278 animals with two AWC^{OFF} neurons decreased (Figure 4E). Secondly, we found that
279 overexpression of *str-130* in *nsy-1* mutant animals inhibited SS digestion, thereby
280 slowing animal growth (Figure 4F), and the proportion of animals with two AWC^{OFF}
281 neurons increased (Figure 4G). These results demonstrate that NSY-1 promotes the
282 AWC^{OFF} state by inducing *str-130* expression, which in turn inhibits SS digestion in *C.*
283 *elegans*.

284 To definitively establish the epistatic relationship between NSY-1 and STR-130, we
285 performed RNAi knockdown of *str-130* in the *nsy-1(ag3)* mutant background and
286 assessed development on SS food. We found that the *str-130* RNAi did not further
287 enhance the developmental capacity of *nsy-1(ag3)* mutant animals on SS (Figure
288 4—figure supplement 3). This epistasis confirms STR-130 functions strictly
289 downstream of NSY-1 within the same genetic pathway. Together with our
290 overexpression data (Figure 4F-G) showing neuronal *str-130* rescue suppresses SS

291 digestion in *nsy-1* mutants, these results establish a linear signaling axis where NSY-1
292 primarily achieves functional inhibition of SS digestion through induction of the
293 GPCR *str-130*.
294

295

296 **NSY-1 Mutation Promotes SS Digestion by Inducing Insulin Signaling**

297 NSY-1 mutation promotes the digestion of unfavorable food, such as SS, and supports
298 *C. elegans* growth (Figure 2A). We hypothesize that, in addition to upregulating
299 certain genes, such as *str-130*, to inhibit SS digestion, NSY-1 may also suppress
300 certain genes to prevent nematodes from utilizing SS (Figure 5A). One possibility is
301 that some genes, induced by the *nsy-1* mutation under SS feeding conditions could
302 facilitate SS digestion in the *nsy-1* mutant (Figure 5A).

303 Our RNA-seq analysis identified 308+46=354 genes that are induced by the *nsy-1*
304 mutation under SS feeding conditions (Figure 5B, Supplementary file 3). However,
305 among these 354 genes, 46 genes can also be induced in wild-type animals fed with
306 SS, suggesting that these 46 genes may not be involved in digesting SS in *nsy-1*
307 mutants. Therefore, the 308 candidate genes induced by the *nsy-1* mutation under SS
308 feeding conditions could potentially promote animals to digest SS.

309 Enrichment analysis revealed that genes related to extracellular functions, such as
310 insulin-related genes, are induced in *nsy-1* mutant animals (Figure 5—figure
311 supplement 1A, Supplementary file 4). Further analysis of insulin-related genes from
312 the RNA-seq data showed that *ins-23* is predominantly induced in *nsy-1* mutant
313 animals (Figure 5—figure supplement 1B), suggesting its potential role in promoting
314 SS digestion.

315 To determine if insulin-like peptide genes were functionally responsible for the
316 enhanced SS growth observed in *nsy-1(ag3)* mutants, we performed functional
317 phenotypic screening using the SS growth assay (worm length assay). We individually
318 knocked down each of these candidates (*ins-22, ins-23, ins-24, ins-27*) in the
319 *nsy-1(ag3)* mutant background. Among these, only RNAi targeting *ins-23*
320 significantly suppressed the enhanced development of the *nsy-1(ag3)* mutant on SS
321 (Figure 5—figure supplement 2, Figure 5D). This targeted functional screening
322 revealed that *ins-23* has the most robust and specific role in mediating the enhanced

digestion phenotype downstream of NSY-1 loss, providing the critical justification for our subsequent focus on this particular insulin-like peptide.

Given that INS-23 is expressed in AWC neurons (Figure 5—figure supplement 3A, from CeNGEN), this suggests increased production and likely enhanced release of INS-23 from AWC neurons in the *nsy-1(ag3)* mutant background, which promotes SS digestion.

The insulin/insulin-like growth factor signaling (IIS) pathway, particularly through the DAF-2 receptor, integrates nutritional signals to regulate various behavioral and physiological responses related to food (Kodama et al., 2006; Ryu et al., 2018). It has been shown that INS-23 acts as an antagonist for the DAF-2 receptor to promote larval diapause (Matsunaga et al., 2018). To test whether *ins-23* induction in *nsy-1(ag3)* mutants promotes SS digestion through its receptor, DAF-2, we constructed a *nsy-1; daf-2* double mutant. We found that the SS digestion ability of the *nsy-1* mutant was inhibited by the *daf-2* mutation (Figure 5E). This suggests that the *nsy-1* mutation induces the insulin peptide *ins-23*, which promotes SS digestion through its potential receptor, DAF-2.

To investigate whether DAF-2 acts as the gut-localized receptor for neuronal INS-23 signaling, we performed tissue-specific rescue experiments in the *nsy-1(ag3);daf-2(e1370)* double mutant. When DAF-2 was re-introduced specifically in the intestine (using the *ges-1* promoter), we observed a significant suppression of SS digestion (Figure 5—figure supplement 3B), but not rescue digestive defect. This indicates that INS-23 induction in *nsy-1* mutants promotes digestion independently of intestinal DAF-2 function.

As established in our prior work (Geng et al., 2022), SS exposure triggers phosphorylation of PMK-1 (P-PMK-1) in *C. elegans*, and *pmk-1* mutants exhibit enhanced growth on SS. This confirms that PMK-1-mediated innate immune signaling actively regulates SS responsiveness and digestion. To address whether PMK-1 functions downstream of NSY-1 within our proposed model, we performed critical epistasis analyses. While we observed that *nsy-1* mutation elevates *ins-23* (indicating NSY-1 suppression of *ins-23*), knockdown of *pmk-1* did not alter *ins-23* expression levels (Figure 5-figure supplement 3C). This demonstrates that PMK-1

356 does not operate through the INS-23 pathway to regulate SS digestion. Thus, although
357 both pathways respond to SS, the PMK-1-mediated innate immune response and the
358 NSY-1/INS-23 axis constitute distinct regulatory mechanisms governing digestive
359 adaptation.

360 **NSY-1 Mutation Promotes SS Digestion through Regulation of Intestinal BCF-1**

361 In our previous study, we found that heat-killed *E. coli* promotes SS digestion in *C.*
362 *elegans* (Geng et al., 2022), a process requiring intestinal BCF-1 (Hao et al., 2024). In
363 the absence of BCF-1, the digestive capability of the animals is significantly reduced
364 (Hao et al., 2024). This led us to investigate whether NSY-1 in AWC neurons
365 regulates intestinal *bcf-1* expression.

366 Firstly, we used a BCF-1::GFP reporter to measure *bcf-1* expression in *nsy-1* mutant
367 animals. We found that mutation of *nsy-1* induced *bcf-1* expression in animals fed
368 either SS or OP50 food (Figure 6A). Additionally, we confirmed that *nsy-1* mutation
369 in AWC neurons also induced intestinal *bcf-1* expression under SS feeding conditions
370 (Figure 6B). This data indicates that NSY-1 in AWC neurons inhibits intestinal *bcf-1*
371 expression, implying that *nsy-1* mutation promotes SS digestion through BCF-1.

372 Next, we constructed a *nsy-1; bcf-1* double mutant and analyzed the growth of these
373 animals on SS. We found that the digestive ability of *nsy-1* mutants was inhibited by
374 the mutation of *bcf-1* (Figure 6C). Together, our data suggest that the increased
375 digestion ability in *nsy-1* mutant animals is dependent on the intestinal digestion
376 factor BCF-1

377 We then asked how *nsy-1* regulates intestinal *bcf-1* expression. Since *nsy-1* mutation
378 induces the insulin peptide *ins-23*, which promotes SS digestion, we tested whether
379 the induction of intestinal *bcf-1* by *nsy-1* mutation is also mediated through INS-23.
380 We found that the *bcf-1*::GFP level decreased in *nsy-1* mutant animals following
381 *ins-23* RNAi treatment (Figure 6D). This suggests that *nsy-1* mutation activates *bcf-1*
382 expression in the intestine, which requires INS-23.

383 To test whether INS-23 acts in AWC neurons to regulate intestinal BCF-1, we
384 generated AWC-specific knockdown strains which was achieved by rescuing *sid-1*
385 cDNA expression under the *ceh-36* promoter in a *sid-1(qt9)*;BCF-1::GFP background.
386 We found that AWC-restricted *ins-23* knockdown significantly reduced intestinal
387 BCF-1::GFP expression (Figure 6—figure supplement 1A). This confirms that

INS-23 functions within AWC sensory neurons to activate intestinal BCF-1, consistent with NSY-1's upstream inhibition of INS-23 in this neuronal subtype.

NSY-1 promotes the AWC^{OFF} state through STR-130 to suppress SS digestion. To determine whether AWC-expressed STR-130 regulates intestinal BCF-1 expression, We observed that AWC neuron-specific RNAi of *str-130* elevated intestinal BCF-1::GFP expression (Figure 6—figure supplement 1B). This demonstrates that STR-130 functions in AWC neurons to repress BCF-1 expression in the intestine.

Discussion

This study in *Caenorhabditis elegan*s reveals a neural-digestive mechanism for evaluating harmful food (Figure 7). The neuron-expressed NSY-1 protein detects *Staphylococcus saprophyticus* (SS) as unsafe food, triggering a digestive shutdown via the AWC^{OFF} neural circuit and the NSY-1-dependent STR-130. Mutations in NSY-1 lead to SS digestion, activating the insulin/IGF-1 signaling (IIS) pathway and BCF-1 expression. These findings highlight a food quality evaluation strategy where neurons communicate with the digestive system to assess food safety, providing insights into how animals adapt to toxic food environments.

The identification of NSY-1 in AWC neurons as a key player in detecting *Staphylococcus saprophyticus* (SS) and initiating digestive shutdown is particularly intriguing. NSY-1, a MAP kinase (MAPKKK), is known to regulate the asymmetric expression of odorant receptors, contributing to neuronal asymmetry and diversity (Chuang and Bargmann, 2005; Chuang et al., 2007; Sagasti et al., 2001; Troemel et al., 1999). Previous research has demonstrated that AWC neurons are pivotal in chemotaxis and sensory processing (Bargmann et al., 1993; Troemel et al., 1997; Wes and Bargmann, 2001) . Our findings extend its function to include food quality assessment, showing that NSY-1 can trigger a digestive shutdown via the AWC^{OFF} neural circuit.

This neural circuit appears to be a crucial component of a systemic food quality control mechanism, allowing animals to adapt effectively to harmful food sources. The state of AWC neurons (AWC^{ON} or AWC^{OFF}) directly influences the animal's ability to digest SS, with the AWC^{OFF} state inhibiting digestion and the AWC^{ON} state promoting it. The finding that activation of the AWC^{OFF} neural circuit leads to a

422 systemic digestive shutdown mediated by NSY-1-dependent GPCR(STR-130) is
423 another notable advancement. GPCRs are well-known for their roles in sensory
424 perception (Julius and Nathans, 2012; Troemel et al., 1995). Our results suggested
425 that GPCR STR-130 play a role in shutting down digestive processes though
426 maintaining AWC^{OFF} states for evaluating harmful food.

427 Our study underscores the critical role of insulin signaling pathways in mediating the
428 effects of neuronal detection on intestinal functions. Upon detection of SS by AWC
429 neurons, NSY-1 inhibits the expression of insulin-like peptides, particularly INS-23.
430 These neuronal peptides promotes the expression of BCF-1, a key regulatory factor in
431 digestion (Hao et al., 2024). Once *ins-23* was inhibited by neuronal NSY-1, the
432 intestinal BCF-1 level is also reduced, which in turn shutdown digestion. We found
433 that the digestive ability of *nsy-1* mutants was totally inhibited by the mutation of
434 *bcf-1* (Figure 6C), suggest that the increased digestion ability in *nsy-1* mutant animals
435 is mainly dependent on the intestinal digestion factor BCF-1. This regulatory cascade
436 highlights the intricate link between neuronal signals and gut responses, ensuring an
437 adaptive reaction to harmful food. We speculated that except INS-23, there should be
438 other factors as signaling regulated by neuronal NSY-1 to inhibits intestinal digestion
439 factor BCF-1 for digestion shutdown.

440 Future studies should focus on delineating the precise molecular pathways linking
441 NSY-1 signaling in AWC neurons to digestion regulation in the gut. Identifying the
442 role of other sensory neurons in food quality assessment and their interactions with
443 the digestive system may uncover new facets of neuron-gut communication and
444 adaptive responses.

445 In summary, our study reveals a sophisticated mechanism in *C. elegans* that integrates
446 neuronal detection of harmful food sources with systemic digestive responses. This
447 neuron-digestive crosstalk is crucial for maintaining organismal homeostasis and
448 survival in the presence of toxic food sources. The findings suggest that similar
449 pathways may exist in other species, including humans, providing a foundation for
450 future research on food safety, toxin avoidance, and the neural regulation of digestive
451 processes. This has important implications for public health, as it illuminates the
452 biological mechanisms underlying foodborne illness and the body's defenses against
453 such threats.

454

455 **Author Contributions**

Y. L and G.T performed experiments, analyzed data and wrote the paper; Z. W performed phenotype analysis; J. Z performed EMS screen; H. L analyzed EMS sequencing data; S. Z supervised some experiments; Z. S supervised some experiments, wrote and revised this paper; B.Q. supervised this study, and wrote the paper with inputs from G. T and Y. L.

Acknowledgments

We thank the Caenorhabditis Genetics Center (CGC) (funded by NIH P40OD010440) for strains; We thank Dr. Huanhu Zhu and Dr. Xiajing Tong (ShanghaiTech University), Dr. Hongyun Tang (Westlake University), Dr. Zhiyong Shao (Fudan University) for sharing strains. This work was supported by the Yunnan Provincial Science and Technology Project at Southwest United Graduate School (202302AP370005 to B.Q.), Yunnan Applied Basic Research Projects (202201AT070196 to B.Q.), Yunnan Revitalization Talent Support Program (C619300A086 to Z.S., K264202230211 to B.Q.), Ministry of Science and Technology of the People's Republic of China (2019YFA0803100，2019YFA0802100 to B.Q), the National Natural Science Foundation of China (32071129 to Z.S., 32170794 to B.Q.), .

Declaration of interests

The authors declare no competing interests.

<u>Main Figure Legends:</u>

Figure 1. *C. elegans* shuts down its digestion for survival when fed harmful food, specifically *Staphylococcus saprophyticus* (SS).

(A) Microscopic images showing worms fed with SS arrested at the L1 stage three days after hatching.

(B) Schematic model illustrating our hypothesis: *C. elegans* can sense or evaluate inedible food, such as SS, and subsequently shut down their digestion to arrest development as a protective survival strategy.

(C) Schematic drawing and quantitative data of the food dwelling/avoidance assay. Yellow circles indicate the food spot for OP50 or SS bacteria, respectively. The animals were scored at the indicated times after L1 worms were placed on the food spot. The red point indicates the position of each worm. Data are represented as mean ± SD. Scale bar = 1000 μm. ***$p < 0.001$; **$p < 0.01$ by Student's t-test.

493 **(D)** Schematic drawing, microscopic images, and quantitative data of the food choice
494 assay. L1 worms were placed at the center spot (origin). OP50 (yellow) and SS (blue)
495 bacteria were placed on opposite sides of the plate. The red point indicates the
496 position of each worm. The percentage of worms on each spot was calculated at the
497 indicated times. Data are represented as mean ± SD. Scale bar = 1000 μm. ****p <
498 0.0001; **p < 0.01 by Student's t-test.
499 **(E-F)** Schematic drawing and quantitative data of the lifespan of animals fed with SS
500 or OP50. L1 worms were seeded onto OP50 and grown to the L4 stage. L4 worms
501 were then moved to SS or OP50 food to measure lifespan. **p < 0.01 by log-rank test.
502 All data are representative of at least three independent experiments.
503
504 **Figure 2. *C. elegans* senses SS and shuts down digestion through NSY-1.**
505 **(A)** Developmental phenotype of wild-type N2 and *nsy-1(ag3)* mutant worms fed
506 with SS bacteria. Data are represented as mean ± SD. Scale bar = 200 μm. ****p <
507 0.0001 by Student's t-test. n= number of animals which were scored.
508 **(B)** Schematic drawing, microscopic images, and quantitative data of the food
509 dwelling/avoidance assay. Yellow circles indicate the food spot for SS bacteria. The
510 animals were scored at the indicated times after L1 worms were placed on the food
511 spot. The blue circle indicates the edge of the bacterial lawn, and the red point
512 indicates the position of each worm. Data are represented as mean ± SD. Scale bar =
513 1000 μm. *p < 0.05; **p < 0.01 by Student's t-test.
514 **(C)** Schematic drawing, microscopic images, and quantitative data of the food choice
515 assay. L1 *nsy-1(ag3)* worms were placed at the center spot (origin). Heat-killed OP50
516 (yellow) and SS (blue) bacteria were placed on opposite sides of the plate. The red
517 point indicates the position of each worm. The percentage of worms on each spot was
518 calculated at the indicated times. Data are represented as mean ± SD. Scale bar= 1000
519 μm. **p < 0.01; ***p < 0.001 by Student's t-test.
520 **(D)** Survival curves of wild-type N2 and *nsy-1(ag3)* mutant worms fed with SS
521 bacteria. L4 worms, previously fed OP50 bacteria, were transferred to SS food to
522 measure lifespan. ****p < 0.0001 by log-rank test.
523 All data are representative of at least three independent experiments.
524
525 **Figure 3. NSY-1 plays a critical role in AWC neurons to inhibit SS digestion.**
526 **(A)** Microscopic image showing the expression pattern of *nsy-1*. The head of an adult
527 transgenic animal carrying *Pnsy-1::GFP* and *Podr-1::RFP* shows colocalization of
528 *nsy-1* and *odr-1*. Scale bar = 20 μm.
529 **(B)** Developmental progression of *nsy-1(ag3)* mutant worms carrying

530 *Podr-1::nsy-1::gfp* (AWC neuron-specific expression) grown on SS bacteria. Control
531 animals are labeled with white stars, and animals carrying the transgenes (rescued
532 animals) are labeled with yellow stars. Data are represented as mean ± SD. Scale bar=
533 200 μm. ****p < 0.0001 by Student's t-test. n= number of animals which were scored.
534 **(C)** Developmental progression of wild-type N2 and AWC neuron-specific knockout
535 *nsy-1* animals (AWC *nsy-1* KO) grown on SS bacteria. Data are represented as mean
536 ± SD. Scale bar= 500 μm. ***p < 0.001 by Student's t-test. n= number of animals
537 which were scored.
538 **(D)** Microscopic images show P*str-2::GFP*, a marker for AWC neuron states, in
539 L1-staged wild-type and *nsy-1(ky397)* mutant worms grown on OP50 or SS bacteria
540 for 6 hours. AWC neuron positions are highlighted with red and yellow arrows. Scale
541 bar= 20 μm.
542 **(E-F)** Percentage of animals with different AWC neuron states. *nsy-1* mutation
543 promotes an $2AWC^{ON}$ state under SS feeding conditions (E), with approximately 50%
544 of animals exhibiting $2AWC^{OFF}$ neurons when feeding on SS (F). Data are represented
545 as mean ± SD. **p < 0.01 by Student's t-test. n= number of animals which were
546 scored.
547 **(G)** Developmental progression of wild-type N2, *tir-1(qd4)*, and *nsy-1(ag3)* mutant
548 worms grown on SS bacteria. Data are represented as mean ± SD. Scale bar= 200 μm.
549 ****p < 0.0001 by Student's t-test. n= number of animals which were scored.
550 All data are representative of at least three independent experiments.
551
552
553 **Figure 4. NSY-1 inhibits animals from digesting SS by inducing *str-130*.**
554 **(A)** Schematic illustration showing that "X" genes rely on NSY-1 to shut down SS
555 digestion. "X" genes induced by SS food are dependent on NSY-1, and their induction
556 aids in shutting down SS digestion.
557 **(B)** Venn diagram showing the overlap of genes that respond to SS and rely on NSY-1.
558 The number of genes is indicated in the diagram (also see Supplementary file 1).
559 **(C)** Transcriptome analysis showing *str-130* mRNA expression, which relies on
560 NSY-1 in response to SS. Data are represented as mean ± SD. **p < 0.01 by Student's
561 t-test.
562 **(D)** Developmental progression of wild-type animals treated with control RNAi or
563 *str-130* RNAi grown on SS bacteria. Data are represented as mean ± SD. Scale bar=
564 200 μm. ****p < 0.0001 by Student's t-test. n= number of animals which were scored.
565 **(E)** Microscopic images and quantitative data of AWC neuron states in L1 animals
566 treated with control RNAi or *str-130* RNAi grown on SS bacteria. Data are

represented as mean ± SD. Scale bar= 20 μm. ***p < 0.001 by Student's t-test ($1AWC^{ON}/1AWC^{OFF}$: control vs *str-130* RNAi). n= number of animals which were scored.

(F) Developmental progression of *nsy-1(ag3)* mutant worms carrying *Pstr-130::str-130::mCherry* grown on SS bacteria. Control animals are labeled with white stars, and animals carrying transgenes are labeled with yellow stars. Data are represented as mean ± SD. Scale bar= 400 μm. ***p < 0.001 by Student's t-test. n= number of animals which were scored.

(G) Microscopic images and quantitative data of AWC neuron states in L1 animals carrying *Pstr-130::str-130::mCherry*. Transgenic animals with overexpression of *str-130* (carrying *Pord-1::GFP* as a co-injection marker) show an increased $2AWC^{OFF}$ state. Data are represented as mean ± SD. Scale bar= 20 μm. ****p < 0.001 by Student's t-test ($2AWC^{OFF}$: Control vs Transgene). n= number of animals which were scored.

All data are representative of at least three independent experiments.

Figure 5. NSY-1 mutation activates animals to digest SS by inducing insulin signaling.

(A) Schematic illustration showing that NSY-1 inhibits the expression of "Y" genes, which promote SS digestion. Some genes induced by the *nsy-1* mutation under SS feeding conditions could facilitate SS digestion in the *nsy-1* mutant.

(B) Venn diagram showing the overlap of genes that respond to SS but are limited by NSY-1. A total of 308 candidate genes induced by the *nsy-1* mutation under SS feeding conditions could potentially promote SS digestion.

(C) Transcriptome analysis showing that *ins-23* expression is induced in animals with the *nsy-1* mutation under SS feeding conditions. Data are represented as mean ± SD. **p < 0.01; n.s. not significant by Student's t-test. n=three biological replicates.

(D) Developmental progression of *nsy-1(ag3)* mutant animals treated with control RNAi or *ins-23* RNAi grown on SS bacteria. Data are represented as mean ± SD. Scale bar = 500 μm. ****p < 0.0001 by Student's t-test. n= number of animals which were scored.

(E) Developmental progression of *nsy-1(ag3), daf-2(e1370)* and *nsy-1(ag3);daf-2(e1370)* double mutant animals grown on SS bacteria. Data are represented as mean ± SD. Scale bar = 500 μm. ****p < 0.0001 by Student's t-test. n= number of animals which were scored.

All data are representative of at least three independent experiments.

604 **Figure 6. NSY-1 mutation promotes animals to digest SS through inducing**
605 **intestinal *bcf-1*.**
606 **(A)** Microscopic images and quantitative data showing fluorescence of
607 *Pbcf-1::bcf-1::GFP* in L1-staged wild-type (WT) and *nsy-1(ag3)* mutant animals fed
608 with OP50 or SS bacteria for 6 hours. Data are represented as mean ± SD. Scale bar=
609 100 μm. ****p < 0.0001 by Student's t-test. n= number of animals which were
610 scored.
611 **(B)** Microscopic images and quantitative data showing fluorescence of
612 *Pbcf-1::bcf-1::GFP* in L1-staged wild-type and AWC *nsy-1* KO mutant (AWC
613 neuron-specific knockout *nsy-1* animals) fed with SS bacteria for 6 hours. Data are
614 represented as mean ± SD. Scale bar = 50 μm. ****p < 0.0001 by Student's t-test.
615 n= number of animals which were scored.
616 **(C)** Developmental progression of wild-type N2, *nsy-1(ag3), bcf-1(ok2599),* and
617 *nsy-1(ag3);bcf-1(ok2599)* double mutant animals grown on SS bacteria. Data are
618 represented as mean ± SD. Scale bar = 200 μm. ****p < 0.0001 by Student's t-test.
619 n= number of animals which were scored.
620 **(D)** Microscopic images and quantitative data showing fluorescence of
621 *Pbcf-1::bcf-1::GFP* in *nsy-1(ag3)* mutant animals treated with control RNAi or *ins-23*
622 RNAi under normal RNAi feeding conditions. Data are represented as mean ± SD.
623 Scale bar = 200 μm. ****p < 0.0001 by Student's t-test. n= number of animals
624 which were scored.
625 All data are representative of at least three independent experiments.
626
627 **Figure 7. A model reveals a neural-digestive mechanism for evaluating harmful**
628 **food.**
629 **(A)** AWC neuron-expressed NSY-1 detects *Staphylococcus saprophyticus* (SS) as
630 harmful food and shuts down digestion by inducing the AWC^{OFF} neural circuit and
631 NSY-1-dependent STR-130. This mechanism protects animals and helps them avoid
632 harmful food.
633 **(B)** Mutations in NSY-1 lead to SS digestion by activating the insulin/IGF-1 signaling
634 (IIS) pathway and BCF-1 expression, thereby reducing the animals' ability to avoid
635 harmful food and decreasing their protection.
636
637
638 **Supplemental Figure Legends:**
639
640 **Figure 1—figure supplement 1. SS is harmful food that animals cannot digest.**

641 **Related to Figure 1.**
642 **(A)** Schematic drawing, microscopic images, and quantitative data from the food
643 choice assay. L1 worms were placed at the center spot (origin). OP50 (yellow) and
644 heat-killed OP50 (blue) bacteria were positioned on opposite sides of the plate. The
645 red point indicates the position of each worm. The percentage of worms on each spot
646 was calculated at the indicated times. Data are represented as mean ± SD. Scale bar=
647 1000 μm. ****$p < 0.0001$; ***$p < 0.001$; **$p < 0.01$ by Student's t-test.
648 **(B)** Schematic drawing, microscopic images, and quantitative data from the food
649 choice assay. L1 worms were placed at the center spot (origin). Heat-killed OP50
650 (blue) and SS (red) bacteria were positioned on opposite sides of the plate. The red
651 point indicates the position of each worm. The percentage of worms on each spot was
652 calculated at the indicated times. Data are represented as mean ± SD. Scale bar= 1000
653 μm. ****$p < 0.0001$; n.s. not significant by Student's t-test.
654 **(C)** Schematic drawing and quantitative data of the lifespan of animals fed with SS or
655 OP50. L1 worms were seeded on plates with no food (NGM) or SS bacteria to
656 measure lifespan. n.s. not significant by log-rank test.
657 **(D)** Schematic drawing and quantitative data of the developmental progression of
658 wild-type N2 under different feeding conditions. L1 animals were seeded onto OP50
659 plates and grown to the L2 stage. L2 animals were then transferred to OP50, SS, or no
660 food (NGM) plates to measure worm length at the indicated time points.
661 All data are representative of at least three independent experiments.
662
663 **Figure 2—figure supplement 1. EMS screen to identify genes involved in shutting**
664 **down digestion of SS.**
665 **(A)** Schematic illustration of the EMS screen strategy to identify "Y" genes involved
666 in shutting down digestion after sensing SS. In mutants with defects in "Y" genes,
667 digestion of SS is restored, allowing the mutants to grow on SS.
668 **(B)** Developmental phenotype of wild-type N2 and *ylf6* mutant worms fed with SS
669 bacteria. Scale bar = 200 μm.
670 **(C)** Schematic drawing showing the mutation sites in *nsy-1(ylf6)* and *nsy-1(ag3)*.
671
672 **Figure 3—figure supplement 1. Construction of *nsy-1* specific knockout in AWC**
673 **neurons using CRISPR-Cas9. Related to Figure 3.**
674 Representative DNA gels showing NheI digestion of PCR-amplified genomic DNA
675 extracted from wild-type (WT) worms and worms with *nsy-1*-specific knockout in
676 AWC neurons (*odr-1p::Cas9* + *u6p::nsy-1-sg*).
677

Figure 3—figure supplement 2. NSY-1 functions in intestine to shut down SS Digestion.

(A) Microscopic image showing the expression pattern of *nsy-1*. *nsy-1* is mainly expressed in the head neurons and intestine. Scale bar = 50 μm.

(B) Developmental progression of *nsy-1(ag3)* mutant worms carrying *Pvha-6::nsy-1::gfp* (intestine-specific expression) grown on SS bacteria. Control animals are labeled with white stars, and animals carrying the transgenes (rescued animals) are labeled with yellow stars. Data are represented as mean ± SD. Scale bar = 200 μm. ****$p < 0.0001$ by Student's t-test. n= number of animals which were scored.

Figure 3—figure supplement 3. NSY-1 functions in AWC neurons to influences the recognition of SS.

(A) Microscopic images, and quantitative data of the food dwelling/avoidance assay. The animals were scored at the indicated times after L1 worms were placed on the food spot. The blue circle indicates the edge of the bacterial lawn, and the red point indicates the position of each worm. Data are represented as mean ± SD. Scale bar= 500 μm. *$p < 0.05$ by Student's t-test.

(B) Microscopic images, and quantitative data of the food dwelling/avoidance assay. The animals were scored at the indicated times after L1 worms were placed on the food spot. The blue circle indicates the edge of the bacterial lawn, and the red point indicates the position of each worm. Data are represented as mean ± SD. Scale bar = 500 μm. **$p < 0.01$; *$p < 0.05$ by Student's t-test.

(C) Microscopic images, and quantitative data from the food choice assay. L1 worms were placed at the center spot (origin). Heat-killed OP50 and SS bacteria were positioned on opposite sides of the plate. The red point indicates the position of each worm. The percentage of worms on each spot was calculated at the indicated times. Data are represented as mean ± SD. Scale bar= 2 mm. ****$p < 0.0001$; ***$p < 0.001$; **$p < 0.01$ by Student's t-test.

(D) Microscopic images, and quantitative data from the food choice assay. L1 worms were placed at the center spot (origin). Heat-killed OP50 and SS bacteria were positioned on opposite sides of the plate. The red point indicates the position of each worm. The percentage of worms on each spot was calculated at the indicated times. Data are represented as mean ± SD. Scale bar = 2 mm. **$p < 0.01$; *$p < 0.05$; n.s. not significant by Student's t-test.

715 **Figure 3—figure supplement 4. AWC neurons are essential for initiating SS**
716 **digestion.**
717 Developmental phenotype of wild-type N2 and AWC(-) worms fed with SS bacteria.
718 Data are represented as mean ± SD. Scale bar = 500 μm. n.s. not significant by
719 Student's t-test. n= number of animals which were scored.
720
721 **Figure 4—figure supplement 1. *str-130* is induced in wild-type in response to SS,**
722 **dependent on NSY-1.**
723 **(A)** GO enrichment analysis of 304 NSY-1-dependent candidate genes responding to
724 SS (Supplementary file 2). Genes related to sensory perception (*sra-32, str-87, str-112,*
725 *str-130, str-160, str-230*) are highlighted as enriched (red arrow).
726 **(B)** Relative mRNA expression levels of sensory perception-related genes (*sra-32,*
727 *str-87, str-112, str-130, str-160, str-230*) extracted from RNA-seq data. These genes
728 are induced in wild-type N2 animals in response to SS, but their expression is reduced
729 in *nsy-1(ag3)* mutant animals under SS feeding conditions, indicating that the
730 induction of these genes in wild-type in response to SS is dependent on NSY-1.
731
732 **Figure 4—figure supplement 2. *str-130* as the dominant effector of**
733 **NSY-1-mediated SS response regulation.**
734 **(A)** Developmental progression of wild-type animals treated with control RNAi,
735 *str-130* RNAi, *sra-32* RNAi, *str-230* RNAi, *str-87* RNAi, *str-112* RNAi or *str-160*
736 RNAi grown on SS bacteria. Data are represented as mean ± SD. Scale bar = 200 μm.
737 ****p < 0.0001; ***p < 0.001; *p < 0.05; n.s. not significant by Student's t-test
738 (candidate RNAi vs Control RNAi). n= number of animals which were scored.
739 **(B)** Developmental progression of *nsy-1(ag3)* mutant animals treated with control
740 RNAi, *str-130* RNAi, *sra-32* RNAi, *str-230* RNAi, *str-87* RNAi, *str-112* RNAi or
741 str-160 RNAi grown on SS bacteria. Data are represented as mean ± SD. Scale bar=
742 500 μm. n.s. not significant by Student's t-test (candidate RNAi vs Control RNAi). n=
743 number of animals which were scored.
744
745 **Figure 4—figure supplement 3. NSY-1 inhibits SS digestion by inducing GPCR**
746 ***str-130*.**
747 Developmental progression of wild-type or *nsy-1(ag3)* mutant animals treated with
748 control RNAi or *str-130* RNAi grown on SS bacteria. Data are represented as mean ±
749 SD. Scale bar = 200 μm. ****p < 0.0001; n.s. not significant by Student's t-test. n=
750 number of animals which were scored.
751

752 **Figure 5—figure supplement 1. *nsy-1* mutation induces the expression of**
753 **insulin-related genes. Related to Figure 5.**
754 **(A)** GO enrichment analysis of 308 genes induced by the nsy-1 mutation under SS
755 feeding conditions (also see Supplementary file 2).
756 **(B)** Relative mRNA expression levels of insulin-related genes (*ins-23, ins-22, ins-27,*
757 *ins-24*) extracted from RNA-seq data. These genes are upregulated in *nsy-1(ag3)*
758 mutant animals under SS feeding conditions, which may contribute to SS digestion in
759 the *nsy-1* mutant.
760
761 **Figure 5—figure supplement 2. NSY-1 mutation promotes SS digestion by**
762 **inducing *ins-23*.**
763 Developmental progression of *nsy-1(ag3)* mutant animals treated with control RNAi,
764 *ins-22* RNAi; *ins-23* RNAi; *ins-24* RNAi; or *ins-27* RNAi grown on SS bacteria. Data
765 are represented as mean ± SD. Scale bar = 500 μm. ****p < 0.0001; n.s. not
766 significant by Student's t-test (candidate RNAi vs Control RNAi). n= number of
767 animals which were scored.
768
769
770 **Figure 5—figure supplement 3. INS-23 induction in *nsy-1* mutants promotes**
771 **digestion independently of intestinal DAF-2 function.**
772 **(A)** CeNGEN predicts showing the head neurons expression pattern of *ins-23*. *ins-23*
773 is expressed in AWC neurons.
774 **(B)** Developmental progression of *nsy-1(ag3);daf-2(e1370)* mutant worms carrying
775 *Pges-1::daf-2::gfp* (intestine-specific expression) grown on SS bacteria. Control
776 animals are labeled with white stars, and animals carrying the transgenes (rescued
777 animals) are labeled with yellow stars. Data are represented as mean ± SD. Scale
778 bar = 200 μm. ****p < 0.0001 by Student's t-test. n= number of animals which were
779 scored.
780 **(C)** Microscopic images and quantitative data showing fluorescence of
781 P*ins-23::ins-23::GFP* animals treated with control RNAi or *pmk-1* RNAi. Data are
782 represented as mean ± SD. Scale bar = 10 μm. n.s. not significant by Student's t-test.
783 n= number of animals which were scored.
784
785
786 **Figure 6—figure supplement 1. INS-23 and STR-130 are functions in AWC**
787 **neurons to affect BCF-1 expression.**
788 **(A)** Microscopic images and quantitative data showing fluorescence of

Pbcf-1::bcf-1::GFP animals treated with control RNAi or AWC *ins-23* RNAi. Data are represented as mean ± SD. Scale bar= 100 μm. ****p < 0.0001 by Student's t-test. n= number of animals which were scored.

(B) Microscopic images and quantitative data showing fluorescence of *Pbcf-1::bcf-1::GFP* animals treated with control RNAi or AWC *str-130* RNAi. Data are represented as mean ± SD. Scale bar= 100 μm. **p < 0.01 by Student's t-test. n= number of animals which were scored.

Supplementary file legends:

Supplementary file 1. List of genes induced by SS food that are dependent on NSY-1. Related to Figure 4B.

Supplementary file 2. GO enrichment analysis of 304 NSY-1-dependent candidate genes responding to SS. Related to Figure 4—figure supplement 1A and B.

Supplementary file 3. List of genes induced in *nsy-1(ag3)* mutant animals feeding on SS. Related to Figure 5B.

Supplementary file 4. GO enrichment analysis of 308 genes induced by the nsy-1 mutation under SS feeding conditions. Related to Figure 5—figure supplement 1A and B.

Star Methods

Resource Availability

Lead contact

Further information and requests for reagents may be directed to the Lead contact Bin Qi (qb@yun.edu.cn).

Materials availability

All reagents and strains generated by this study are available through request to the lead contact with a completed Material Transfer Agreement.

Data and code availability

This paper does not report original code.

Any additional information required to reanalyze the data reported in this paper is available from the lead contact upon request (qb@ynu.edu.cn).

826

827 **Experimental model and subject details**

828

829 ***C. elegans* strains and maintenance**

830 Nematode stocks were maintained on nematode growth medium (NGM) plates seeded
831 with bacteria (*E. coli* OP50) at 20˚C.
832 The following strains/alleles were obtained from the Caenorhabditis Genetics Center
833 (CGC) or as indicated:

834

835 1) The following strains were obtained from CGC:
836 N2 Bristol (wild-type control strain);
837 AU3: *nsy-1(ag3)*;
838 ZD101: *tir-1(qd4)*;
839 RB1971: *bcf-1(ok2599)*;
840 KU25: *pmk-1(km25)*;
841 KU4: *sek-1(km4)*;
842 PY7502: *oyIs85[ceh-36p::TU#813 +ceh-36p::TU#814 + srtx-1p::GFP + un*
843 *c-122p::DsRed]*
844 CB1370: *daf-2(e1370)*; shared from mintie Pu lab
845 CX3695: *str-2::gfp+lin-15(+)*; shared from Huanhu Zhu lab
846 CX4998: *str-2::gfp+lin-15(+);nsy-1(ky397)*; shared from Hongyun Tang lab

847

848 2) The following strains were obtained from published papers.
849 PHX4067: [*Pbcf-1::bcf-1::gfp::3xflag*](He et al., 2023);

850

851 3) **The following strains were constructed by this study:**
852 YNU186: *ylfEx124*[*Pnsy-1::gfp*;*Podr-1::rfp*] was constructed by injecting
853 plasmid *Pnsy-1::nsy-1::gfp* with *Podr-1::rfp* in N2 background;
854 YNU189: *Pbcf-1::bcf-1::gfp::3xflag;nsy-1(ag3)* was constructed by crossing PHX
855 4067[*Pbcf-1::bcf-1::gfp::3xflag*] with AU3[*nsy-1(ag3)*];
856 YNU238: *ylf6(nsy-1*, EMS mutant*)*;
857 YNU465: *ylfEx252*[*Podr-1::nsy-1::gfp;Podr-1::rfp;nsy-1(ag3)*] was constructed by
858 injecting plasmid *Podr-1::nsy-1::gfp* with *Podr-1::rfp* in *nsy-1(ag3)* background;
859 YNU466: *ylfEx253*[*Pvha-6::nsy-1::gfp;Podr-1::rfp;nsy-1(ag3)*] was constructed
860 by injecting plasmid *Pvha-6::nsy-1::gfp* with *Podr-1::rfp* in *nsy-1(ag3)* backgrou
861 nd;
862 YNU488: *ylfEx259*[*Pstr-130::str-130::mcherry*;*Podr-1::rfp*;*nsy-1(ag3)*] was

863 constructed by injecting plasmid *Pstr-130::str-130::mcherry* with *Podr-1::rfp* in
864 *nsy-1(ag3)* background;
865 YNU491: *ylf57*, AWC neuron specific knock out *nsy-1* strain was constructed by
866 injecting plasmid pDD162[P*odr-1::Cas9*+P*u6::nsy-1-sg*], *nsy-1* repair template
867 (synthesis from Tsingke), pDD162[P*eft-3::Cas9*+ P*u6::dpy-10-sg*], dpy-10 repair
868 template(synthesis from Tsingke) in PHX4067(P*bcf-1::bcf-1::gfp::3xflag*)
869 background;
870 YNU501: *nsy-1(ag3)*;*bcf-1(ok2599)* double mutant was constructed by
871 crossing RB1971[*bcf-1(ok2599)*] with AU3[*nsy-1(ag3)*];
872 YNU508: *ylfEx266*[*Pstr130::str-130::mcherry;Podr-1::rfp;nsy-1(ag3)*] was
873 constructed by injecting plasmid *Pstr130::str-130::mcherry* with *Podr-1::rfp* in
874 *str-2::gfp+lin-15(+)* background;
875 YNU517: *nsy-1(ag3);daf-2(e1370)* double mutant was constructed by crossing
876 CB1370[*daf-2(e1370)*] with AU3[*nsy-1(ag3)*];
877 YNU729: *ylfEx351*[*Pges-1::daf-2::gfp*;*Podr-1::rfp*;*nsy-1(ag3);daf-2(e1370)*] was c
878 onstructed by injecting plasmid *Pges-1::daf-2::gfp* with *Podr-1::rfp* in *nsy-1(ag*
879 *3);daf-2(e1370)* background;
880 YNU732: *ylfIs48*[*Podr-1::nsy-1::gfp;Podr-1::rfp;nsy-1(ag3)*] was constructed by
881 injecting plasmid *Podr-1::nsy-1::gfp* with *Podr-1::rfp* in *nsy-1(ag3)* background;
882 YNU730: *ylfEx352*[*Pceh-36::sid-1::mcherry;pRF4(rol-6);Pbcf-1::bcf-1::gfp::3xflag;*
883 *sid-1(qt9)*] was constructed by injecting plasmid *Pceh-36::sid-1::mcherry* with
884 *pRF4(rol-6)* in *Pbcf-1::bcf-1::gfp::3xflag;sid-1(qt9)* background.
885 YNU731: *ylfEx353*[*Pins-23::ins-23::gfp;Podr-1::rfp*] was constructed by injecting
886 plasmid *Pins-23::ins-23::gfp* with *Podr-1::rfp* in N2 background;
887
888
889 **Bacteria Strains**
890 *E. coli*-OP50 (from Caenorhabditis Genetics Center (CGC)), and *Staphylococcus.*
891 *Saprophyticus* (from ATCC) were cultured at 37°C in LB medium. A standard
892 overnight cultured bacteria was then spread onto each Nematode growth media
893 (NGM) plate.
894
895 **Method Details**
896
897 **Generation of transgenic strains**
898 1）To construct the *C. elegans* plasmid for expression of *nsy-1*, 1527bp promoter of
899 *nsy-1* was inserted into the pPD95_77-gfp vector. DNA plasmid mixture containing

P*nsy-1::GFP* (20ng/ul) and P*odr-1p::RFP*(50ng/ul) was injected into the gonads of adult wild-type N2 animals.

2）To construct the *C. elegans* plasmid for expression of *nsy-1* in AWC neuron, 1348bp promoter of *odr-1* and genomic DNA of *nsy-1* was inserted into the pPD49.26-gfp vector. DNA plasmid mixture containing P*odr-1::nsy-1::GFP* (20ng/ul) and P*odr-1::RFP* (50ng/ul) was injected into the gonads of adult *nsy-1(ag3)*.

3）To construct the *C. elegans* plasmid for expression of *str-130*, 2000bp promoter of *str-130* and 1324bp genomic DNA of *str-130* was inserted into the pPD49.26-mcherry vector. DNA plasmid mixture containing P*str-130::str-130::mcherry*(20ng/μl) and P*odr-1::rfp* (50ng/μl) was injected into the gonads of adult CX3695[*str-2::gfp+lin-15(+)*].

4）To construct the *C. elegans* plasmid for expression of *daf-2* in intestine, 2549bp promoter of *ges-1* and 5400bp cDNA of *daf-2* was inserted into the pPD95_77-gfp vector. DNA plasmid mixture containing P*ges-1::daf-2::gfp*(20ng/μl) and P*odr-1::rfp* (50ng/μl) was injected into the gonads of adult *nsy-1(ag3);daf-2(e1370)*.

5）To construct the *C. elegans* plasmid for expression of *sid-1* in AWC neuron, 2000bp promoter of *ceh-36* and 2328bp cDNA of *sid-1* was inserted into the pPD49.26-mcherry vector. DNA plasmid mixture containing P*ceh-36::sid-1::mcherry*(20ng/μl) and *rol-6* (50ng/μl) was injected into the gonads of adult *Pbcf-1::bcf-1::gfp::3xflag;sid-1(qt9)*.

6）To construct the *C. elegans* plasmid for expression of *ins-23*, 2017bp promoter of *ins-23* and 286bp genomic DNA of *ins-23* was inserted into the pPD49.26-gfp vector. DNA plasmid mixture containing P*iins-23::ins-23::gfp*(20ng/μl) and P*odr-1::rfp* (50ng/μl) was injected into the gonads of adult wild-type N2 animals.

Generation *nsy-1* AWC neuron specific knock out strain and Genotyping.

To construct the *C. elegans* plasmid for knock out of *nsy-1* in AWC neuron, 600bp promoter of *eft-3* was replaced by 1348bp promoter of *odr-1* and *nsy-1* sgRNA was also inserted into the same CRISPR-Cas9-sgRNA vector pDD162 (Dickinson et al., 2013). The Cas9 target sites were designed via CRISPR design tool (http://crispor.tefor.net/) and the sgRNA sequences was 5'-GAATTTACGCGTTCGAGAAATGG-3'. Knockout strains were generated by injecting 25ng/μl Cas9-sgRNA plasmid, 2μM repair template, co-injection markers include 20ng/μl *dpy-10* Cas9-sgRNA plasmid and 2μM *dpy-10* repair template.

Worms were picked into 10 μl of worm lysis buffer (50 mM KCl,10 mM Tris-HCl pH 8.0, 2.5 mM $MgCl_2$, 0.45% NP40, 0.45% Tween-20, 0.01% Gelactin, 0.2 mg/mL Proteinase K), quickly freeze-thaw three times using liquid nitrogen,

incubated it at 60°C for 90min and 95 °C for 20min. 1μl supernatant was taken and performed for PCR analysis with the following primers:

nsy-1: forward 5′-CAAGAGGCAAGTGCAGCATA-3′, reverse 5′-TGACTGTCCCATGCTCTCAC-3′, then digested with NheI endonuclease overnight and identified by DNA agarose electrophoresis.

Preparation of *Staphylococcus. Saprophyticus* (SS)

SS preparation was followed by our published protocol (Geng et al., 2022; Liu and Qi, 2023). Briefly, a standard overnight culture of SS (37℃ in LB broth) was diluted into fresh LB broth (1:100ratio). SS was then spread onto each NGM plate when the diluted bacteria grew to OD600 = 0.5.

Analysis of worm's growth in SS bacteria

The standard overnight cultured SS was then spread onto 60mm NGM plate. Worms were grown on *E. coli*-OP50, and eggs were collected by bleaching and then washing in M9 buffer. Synchronized L1 larvae were obtained by allowing the eggs to hatch in M9 buffer for 12 hr. Synchronized L1s were seeded to plates prepared for the specific assay and incubated at 20℃ for 4 days. The developmental conditions were determined by body length.

Food behavior assay

1) Food avoidance assay

Food avoidance assay was performed following to our published methods (Qi et al., 2017). Briefly, 5ul of overnight cultured bacteria was seeded on the center of 60mm NGM plates. About 30-50 synchronized L1 animals were seeded onto the bacterial lawns and cultured at 20℃ for 8hr. The aversion index was determined by N(out of lawn)/N(total).

2) Food choice assay

Food choice assay was performed following to our published methods (Qi et al., 2017). Briefly, 5ul of overnight cultured bacteria was seeded on the different side of 60mm NGM plates. About 300 synchronized L1 animals were seeded onto the center of NGM plates and cultured at 20℃ for 8hr. The food trend index was determined by N (selecting food1)/ [N(selecting food1)+N(selecting food2)] and N(selecting food2)/[N(selecting food1)+N(selecting food2)].

Lifespan analysis

974 **Larval Lifespan**
975 Studies of larval lifespan were performed on NGM plates at 20°C as previously
976 described (Cui et al., 2013). Briefly, L1 staged worms were placed NGM plates or SS
977 seeded NGM plates. Worms were scored every day. Prism8 software was used for
978 statistical analysis.
979 **Adult Lifespan**
980 Studies of lifespan were performed on NGM plates at 20°C as previously described
981 (Kimura et al., 1997).
982 Briefly, lifespan was begun on day zero by placing healthy L4 stage hermaphrodites
983 onto OP50 seeded NGM plates. Animals were transferred to a fresh OP50 or SS
984 seeded plates during the reproductive period (approximately the first ten days) to
985 eliminate self-progeny and every 2 days thereafter. Worms were scored every day.
986 Prism8 software was used for statistical analysis.
987
988 **EMS mutagenesis**
989 Synchronized L1 animals were grown to the L4 stage on OP50 and then subjected to a
990 4-hour treatment with 0.5% EMS (Ethyl Methanesulfonate). After treatment, the P0
991 generation animals were thoroughly washed with M9 solution and transferred to
992 OP50 plates to grow and produce the F1 generation. Groups of 3-4 F1 animals were
993 picked and placed onto new OP50 plates (3-4 F1 worms per plate) to generate the F2
994 generation through self-fertilization. Once the F2 generation reached adulthood, all
995 the F2 animals were bleached to obtain the next generation of eggs. Synchronized L1
996 larvae were obtained by allowing the eggs to hatch in M9 buffer for 12 hours. The
997 synchronized L1s were then seeded onto SS plates and incubated at 20°C for 4 days.
998 Candidate mutants that could grow on SS plates were identified. To confirm the
999 suspected mutants, each candidate mutant was picked singly onto OP50 for passaging
1000 and growth to adulthood. These adult animals were then bleached to obtain
1001 synchronized L1 mutants. The synchronized L1 mutants were seeded onto SS plates
1002 to confirm their ability to grow on SS.
1003 **Identification of EMS mutants**
1004 DNA isolation, library construction, and whole genome sequencing with gene
1005 identified were carried out according to the published protocol (Joseph et al., 2018).
1006 **i) Preparation of samples for Whole-Genome-Sequencing (WGS)**
1007 For each backcross, wild-type males were crossed to mutant hermaphrodites, F1
1008 cross-progeny animals were individually cloned and F2 variants and wild-types were

1009 isolated under SS feeding conditon. The variant strains and wild-type strains were
1010 mixed respectively to constitute the "DNA-pool" used as samples for WGS.
1011 Whole-genome sequencing of pooled F2 recombinants, homozygous for the mutant
1012 phenotype following two outcrosses to wild-type N2 animals, was performed to
1013 identify the mutations.
1014
1015 **ii) WGS data processing**
1016 For Whole-Genome-Sequencing, paired-end libraries were sequenced on an Illumina
1017 HiSeq 2000. Fastqc was used to control the quality of raw data and Trimmomatic was
1018 used to filter the data. Bwa was used to construct the index of *C.elegans* genome and
1019 align clean reads to the reference gene sequence (Species: *Caenorhabditis_elegans*;
1020 Source: UCSC; Reference Genome Version: WBcel235/ce11). The Samtools was used
1021 for file format conversion and sorting. Picard was used to remove the duplicate reads
1022 and then GATK was used to identify the intervals and realign. The realigned sequence
1023 was piled up by Samtools and then inputted to Varscan to call the variants including
1024 SNPs and INDELs. Vcflib was used to perform subtraction between the wild-types
1025 and variants. The file was annotated by Snpeff and the candidate genes was finally
1026 obtained.
1027
1028
1029 **Preparation of samples for RNA sequencing**
1030 RNA-seq was done with three biological replicates that were independently generated,
1031 collected, and processed. Adult wild type (N2) or *nsy-1* mutant worms were bleached
1032 and then the eggs were incubated in M9 for 18 hours to obtain synchronized L1
1033 worms. Synchronized L1 worms were cultured in the NGM plate seeded with OP50
1034 or SS for 4hrs at 20°C. L1 worms were then collected for sequencing.
1035
1036 **Fluorescence microscopy of *C. elegans***
1037 Slides for imaging were prepared by making a fresh flattened 5% agarose pad. Worms
1038 were mounted on 5% agar pads in M9 buffer with 5mM levamisolem then sealed
1039 beneath a 22x22mm coverglass. Imaging was done using an Olympus BX53
1040 microscope with a DP80 camera. *str-2::gfp* or *bcf-1::gfp* expression was measured
1041 through imaging.
1042
1043 **Microscopy**

The fluorescence photographs were taken by Olympus BX53 microscope with a DP80 camera. Development statistics were taken by Olympus MVX10 dissecting microscope with a DP80 camera.

QUANTIFICATION AND STATISTICAL ANALYSIS

Quantification

Animals were randomly selected for fluorescent photography. The size of transgene worms was photographed by the Nomarski microscope and measured by ImageJ software. ImageJ software was used for quantifying fluorescence intensity of indicated animals, which was then normalized with control group.

Statistical analysis

All experiments were performed independently at least three times with similar results.

All statistical analyses were performed using the unpaired two-tailed Student's test. Statistical parameters are presented as mean ± SD, statistical significance ($P<0.05$, *, $P < 0.01$, **, $P < 0.001$, ***), and "n" (the number of worms counted).
The Log rank (Mantel-Cox) test was used for lifespan assay and the exact p values of statistics for all survival assays are listed in the Figure.

Reference:

Avery, J.A., Liu, A.G., Ingeholm, J.E., Gotts, S.J., and Martin, A. (2021). Viewing images of foods evokes taste quality-specific activity in gustatory insular cortex. Proc Natl Acad Sci U S A *118*.

Bargmann, C.I. (2006). Chemosensation in C. elegans. WormBook, 1-29.

Bargmann, C.I., Hartwieg, E., and Horvitz, H.R. (1993). Odorant-selective genes and neurons mediate olfaction in C. elegans. Cell *74*, 515-527.

Baugh, L.R., and Sternberg, P.W. (2006). DAF-16/FOXO regulates transcription of cki-1/Cip/Kip and repression of lin-4 during C. elegans L1 arrest. Curr Biol *16*, 780-785.

Buck, L., and Axel, R. (1991). A novel multigene family may encode odorant receptors: a molecular basis for odor recognition. Cell *65*, 175-187.

Chuang, C.F., and Bargmann, C.I. (2005). A Toll-interleukin 1 repeat protein at the synapse specifies asymmetric odorant receptor expression via ASK1 MAPKKK signaling. Gene Dev *19*, 270-281.

Chuang, C.F., VanHoven, M.K., Fetter, R.D., Verselis, V.K., and Bargmann, C.I. (2007). An innexin-dependent cell network establishes left-right neuronal asymmetry in

. Cell *129*, 787-799.
Cui, M., Cohen, M.L., Teng, C., and Han, M. (2013). The tumor suppressor Rb critically regulates starvation-induced stress response in C. elegans. Curr Biol *23*, 975-980.
Dickinson, D.J., Ward, J.D., Reiner, D.J., and Goldstein, B. (2013). Engineering the genome using Cas9-triggered homologous recombination. Nat Methods *10*, 1028-+.
Felix, M.A., and Braendle, C. (2010). The natural history of Caenorhabditis elegans. Curr Biol *20*, R965-R969.
Fiala, A. (2007). Olfaction and olfactory learning in Drosophila: recent progress. Curr Opin Neurobiol *17*, 720-726.
Florsheim, E.B., Bachtel, N.D., Cullen, J.L., Lima, B.G.C., Godazgar, M., Carvalho, F., Chatain, C.P., Zimmer, M.R., Zhang, C.L., Gautier, G.*, et al.* (2023). Immune sensing of food allergens promotes avoidance behaviour. Nature *620*, 643-+.
Florsheim, E.B., Sullivan, Z.A., Khoury-Hanold, W., and Medzhitov, R. (2021). Food allergy as a biological food quality control system. Cell *184*, 1440-1454.
Geng, S., Li, Q., Zhou, X., Zheng, J., Liu, H., Zeng, J., Yang, R., Fu, H., Hao, F., Feng, Q.*, et al.* (2022). Gut commensal E. coli outer membrane proteins activate the host food digestive system through neural-immune communication. Cell Host Microbe.
Hao, F.R., Liu, H.M., and Qi, B. (2024). Bacterial peptidoglycan acts as a digestive signal mediating host adaptation to diverse food resources in. Nat Commun *15*.
He, Y., Hao, F., Fu, H., Tian, G., Zhang, Y., Fu, K., and Qi, B. (2023). N-glycosylated intestinal protein BCF-1 shapes microbial colonization by binding bacteria via its fimbrial protein. Cell Rep *42*, 111993.
Hukema, R.K., Rademakers, S., Dekkers, M.P., Burghoorn, J., and Jansen, G. (2006). Antagonistic sensory cues generate gustatory plasticity in Caenorhabditis elegans. Embo J *25*, 312-322.
Joseph, B.B., Blouin, N.A., and Fay, D.S. (2018). Use of a Sibling Subtraction Method for Identifying Causal Mutations in Caenorhabditis elegans by Whole-Genome Sequencing. G3 (Bethesda) *8*, 669-678.
Julius, D., and Nathans, J. (2012). Signaling by sensory receptors. Cold Spring Harbor perspectives in biology *4*, a005991.
Kim, D.H., Feinbaum, R., Alloing, G., Emerson, F.E., Garsin, D.A., Inoue, H., Tanaka-Hino, M., Hisamoto, N., Matsumoto, K., Tan, M.W.*, et al.* (2002). A conserved p38 MAP kinase pathway in Caenorhabditis elegans innate immunity. Science *297*, 623-626.
Kimura, K.D., Tissenbaum, H.A., Liu, Y.X., and Ruvkun, G. (1997). daf-2, an insulin receptor-like gene that regulates longevity and diapause in Caenorhabditis elegans. Science *277*, 942-946.
Kodama, E., Kuhara, A., Mohri-Shiomi, A., Kimura, K.D., Okumura, M., Tomioka, M., Iino, Y., and Mori, I. (2006). Insulin-like signaling and the neural circuit for integrative behavior in C. elegans. Genes Dev *20*, 2955-2960.
Liu, H., and Qi, B. (2023). Protocol for investigating the effect of food digestion in C. elegans on development by feeding the inedible bacteria Staphylococcus saprophyticus. STAR Protoc *4*, 101990.
Liu, P., Liu, X., and Qi, B. (2024). UPRER–immunity axis acts as physiological food evaluation system that promotes aversion behavior in sensing low-quality food. Elife *13:RP94181*.
Matsunaga, Y., Matsukawa, T., Iwasaki, T., Nagata, K., and Kawano, T. (2018). Comparison of physiological functions of antagonistic insulin-like peptides, INS-23 and INS-18, in. Biosci Biotech Bioch *82*, 90-96.
McLachlan, I.G., Kramer, T.S., Dua, M., DiLoreto, E.M., Gomes, M.A., Dag, U., Srinivasan, J., and Flavell,

1127 S.W. (2022). Diverse states and stimuli tune olfactory receptor expression levels to modulate
1128 food-seeking behavior. Elife *11*.
1129 Plum, T., Binzberger, R., Thiele, R., Shang, F.W., Postrach, D., Fung, C., Fortea, M., Stakenborg, N., Wang,
1130 Z., Tappe-Theodor, A.*, et al.* (2023). Mast cells link immune sensing to antigen-avoidance behaviour.
1131 Nature *620*, 634-+.
1132 Qi, B., Kniazeva, M., and Han, M. (2017). A vitamin-B2-sensing mechanism that regulates gut protease
1133 activity to impact animal's food behavior and growth. Elife *6*.
1134 Ryu, L., Cheon, Y., Huh, Y.H., Pyo, S., Chinta, S., Choi, H., Butcher, R.A., and Kim, K. (2018). Feeding state
1135 regulates pheromone-mediated avoidance behavior via the insulin signaling pathway in. Embo J *37*.
1136 Sagasti, A., Hisamoto, N., Hyodo, J., Tanaka-Hino, M., Matsumoto, K., and Bargmann, C.I. (2001). The
1137 CaMKII UNC-43 activates the MAPKKK NSY-1 to execute a lateral signaling decision required for
1138 asymmetric olfactory neuron fates. Cell *105*, 221-232.
1139 Samuel, B.S., Rowedder, H., Braendle, C., Felix, M.A., and Ruvkun, G. (2016). Caenorhabditis elegans
1140 responses to bacteria from its natural habitats. P Natl Acad Sci USA *113*, E3941-E3949.
1141 Schulenburg, H., and Felix, M.A. (2017). The Natural Biotic Environment of Caenorhabditis elegans.
1142 Genetics *206*, 55-86.
1143 Scott, K. (2018). Gustatory Processing in Drosophila melanogaster. Annu Rev Entomol *63*, 15-30.
1144 Sengupta, P., Chou, J.H., and Bargmann, C.I. (1996). odr-10 encodes a seven transmembrane domain
1145 olfactory receptor required for responses to the odorant diacetyl. Cell *84*, 899-909.
1146 Troemel, E.R., Chou, J.H., Dwyer, N.D., Colbert, H.A., and Bargmann, C.I. (1995). Divergent seven
1147 transmembrane receptors are candidate chemosensory receptors in C. elegans. Cell *83*, 207-218.
1148 Troemel, E.R., Kimmel, B.E., and Bargmann, C.I. (1997). Reprogramming chemotaxis responses:
1149 sensory neurons define olfactory preferences in C. elegans. Cell *91*, 161-169.
1150 Troemel, E.R., Sagasti, A., and Bargmann, C.I. (1999). Lateral signaling mediated by axon contact and
1151 calcium entry regulates asymmetric odorant receptor expression in C. elegans. Cell *99*, 387-398.
1152 Vidal, B., Aghayeva, U., Sun, H., Wang, C., Glenwinkel, L., Bayer, E.A., and Hobert, O. (2018). An atlas of
1153 Caenorhabditis elegans chemoreceptor expression. Plos Biol *16*, e2004218.
1154 Wes, P.D., and Bargmann, C.I. (2001). odour discrimination requires asymmetric diversity in olfactory
1155 neurons. Nature *410*, 698-701.
1156

Figure 1

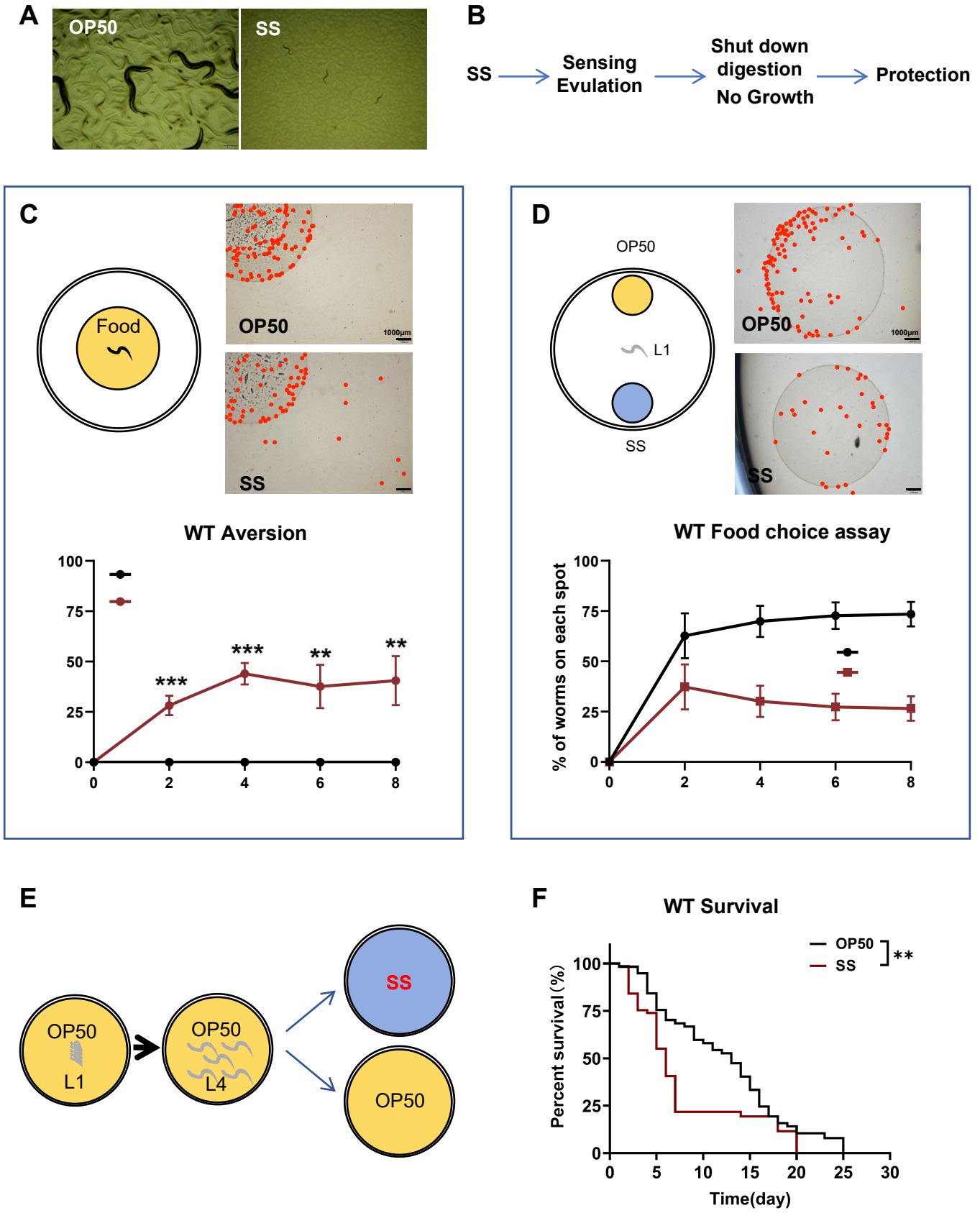
A
OP50
SS
B
SS
Sensing Evulation
Shut down digestion No Growth
Protection
C
Food
OP50
SS
1000μm
WT Aversion
100
75
50
25
0
0
2
4
6
8
***
***
**
**
D
OP50
L1
SS
OP50
SS
1000μm
WT Food choice assay
% of worms on each spot
100
75
50
25
0
0
2
4
6
8
E
OP50
L1
OP50
L4
SS
OP50
F
WT Survival
OP50
SS
**
Percent survival (%)
100
75
50
25
0
0
5
10
15
20
25
30
Time(day)

Figure 2

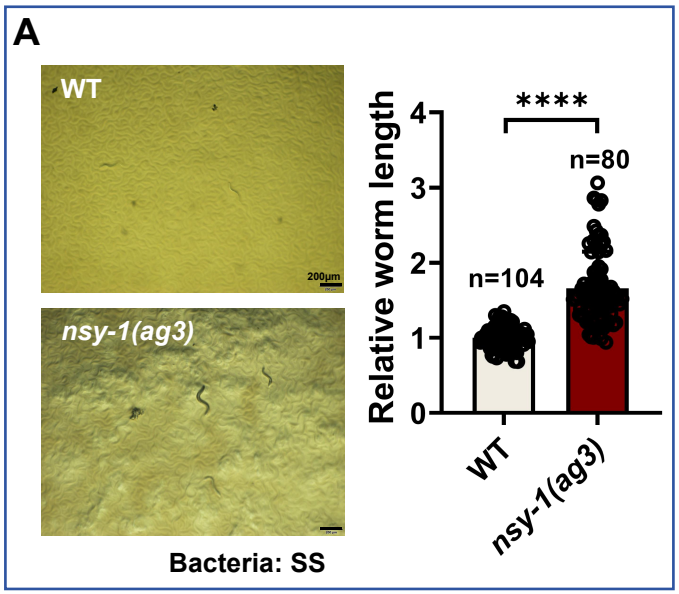
A
WT
200μm
nsy-1(ag3)
Bacteria: SS
Relative worm length
****
n=80
n=104
0
1
2
3
4
WT
nsy-1(ag3)

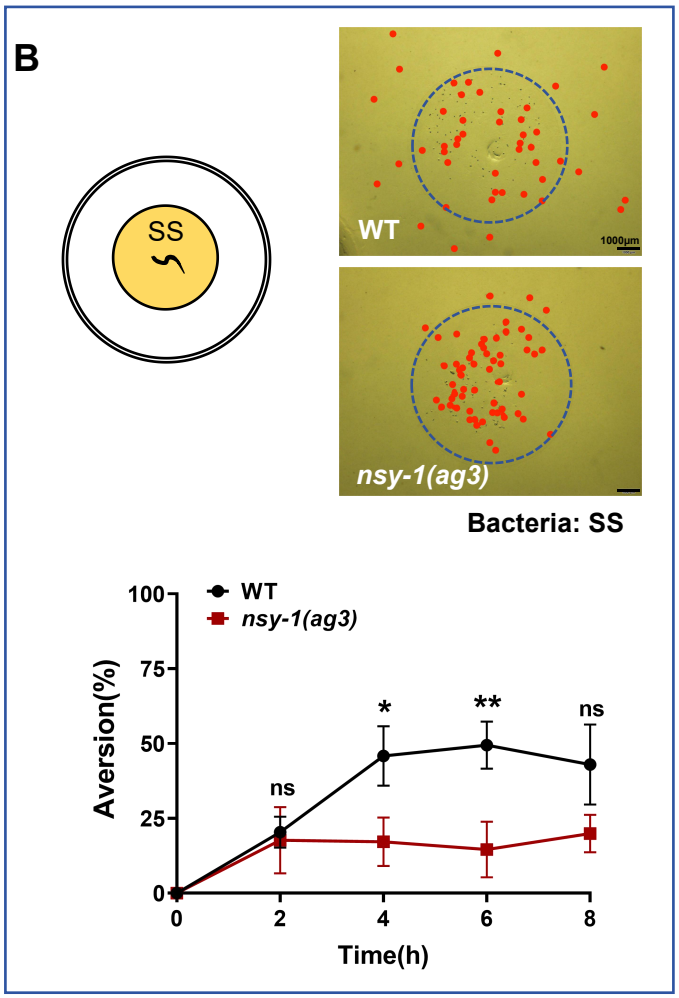
B
SS
WT
1000μm
nsy-1(ag3)
Bacteria: SS
WT
nsy-1(ag3)
Aversion(%)
100
75
50
25
0
ns
*
**
ns
0
2
4
6
8
Time(h)

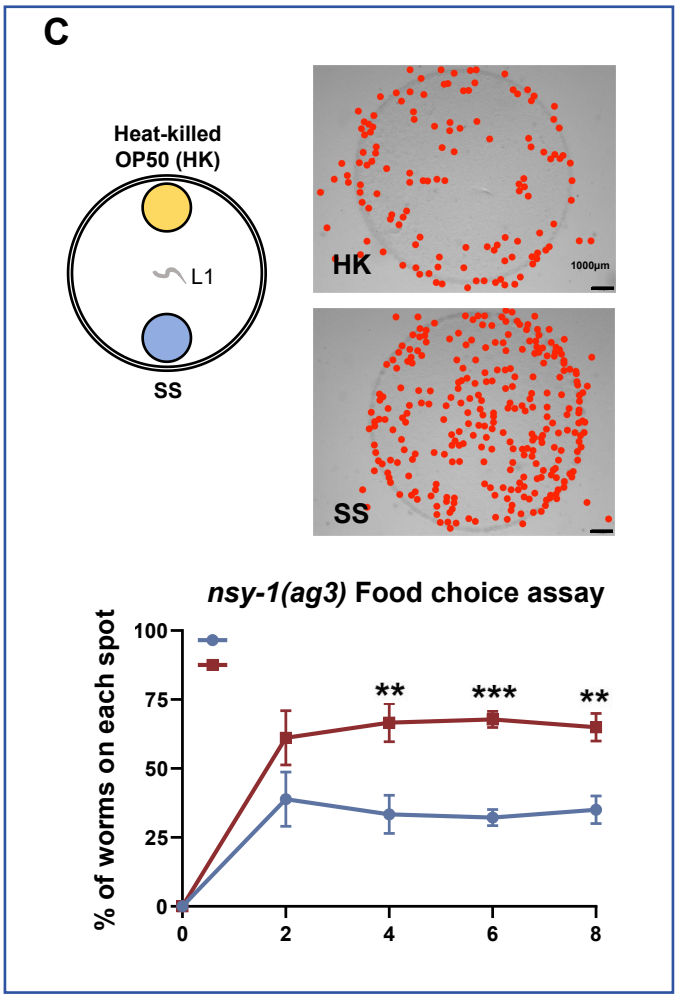
C
Heat-killed
OP50 (HK)
L1
SS
HK
1000μm
SS
nsy-1(ag3) Food choice assay
% of worms on each spot
100
75
50
25
0
**
***
**
0
2
4
6
8

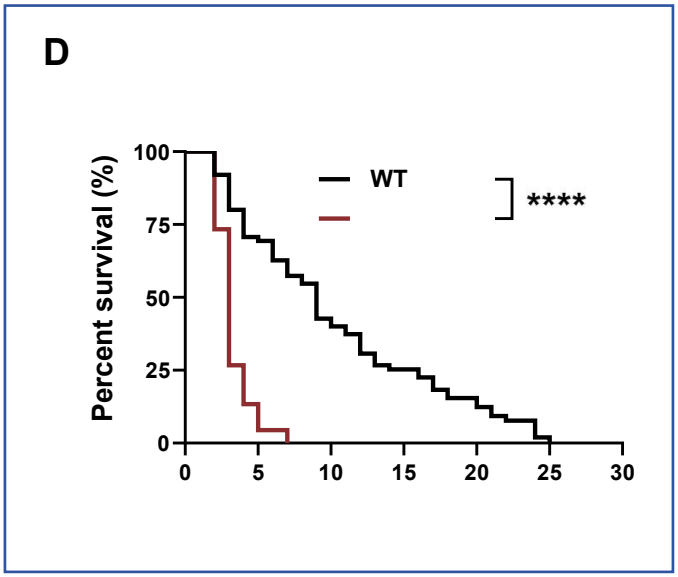
D
Percent survival (%)
100
75
50
25
0
WT
****
0
5
10
15
20
25
30

Figure 3

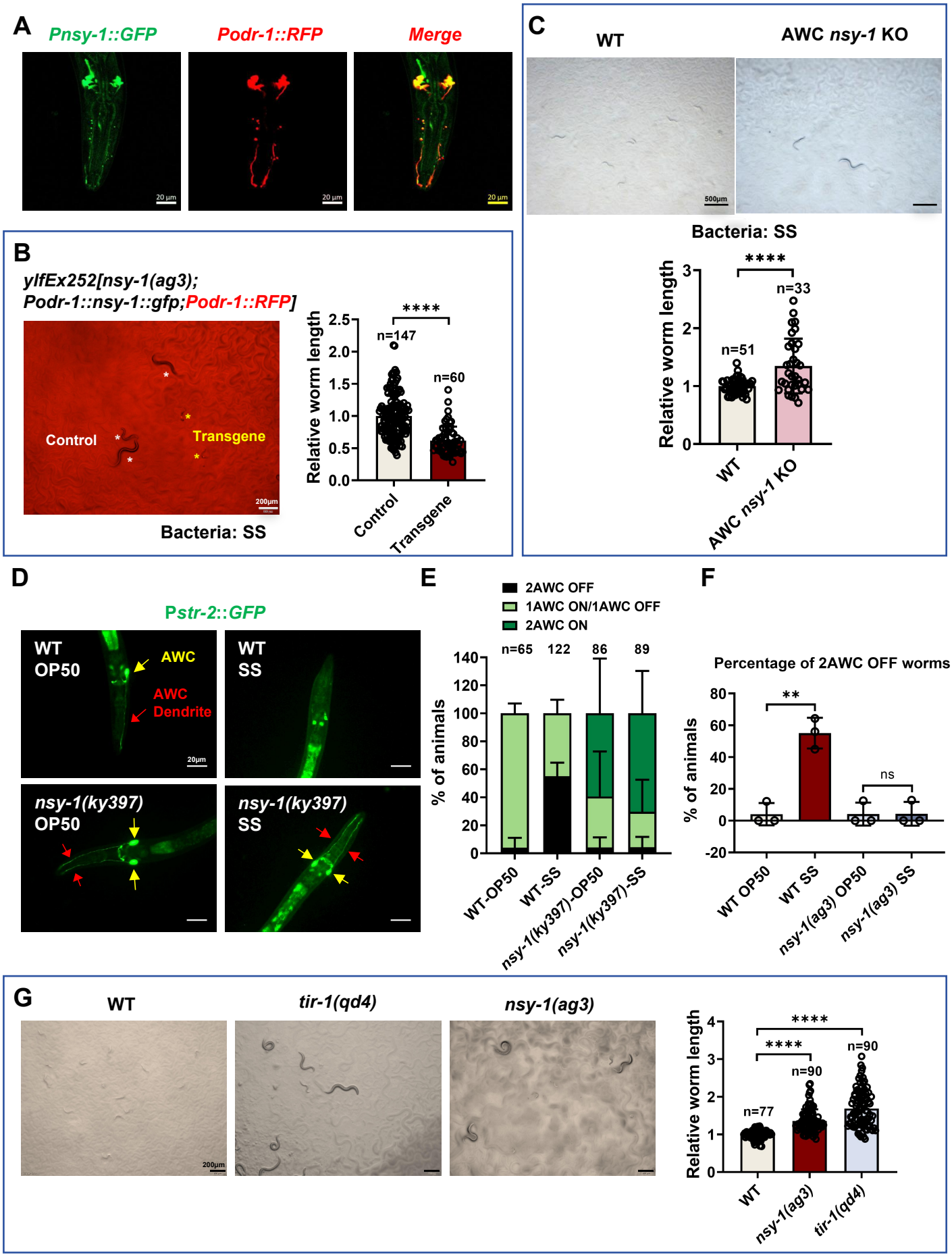
A
Pnsy-1::GFP
Podr-1::RFP
Merge
20 µm
B
ylfEx252[nsy-1(ag3); Podr-1::nsy-1::gfp;Podr-1::RFP]
Control
Transgene
200µm
Bacteria: SS
Relative worm length
****
n=147
n=60
Control
Transgene
C
WT
AWC nsy-1 KO
500µm
Bacteria: SS
Relative worm length
****
n=51
n=33
WT
AWC nsy-1 KO
D
Pstr-2::GFP
WT OP50
AWC
AWC Dendrite
20µm
WT SS
nsy-1(ky397) OP50
nsy-1(ky397) SS
E
2AWC OFF
1AWC ON/1AWC OFF
2AWC ON
n=65 122 86 89
% of animals
WT-OP50
WT-SS
nsy-1(ky397)-OP50
nsy-1(ky397)-SS
F
Percentage of 2AWC OFF worms
% of animals
**
ns
WT OP50
WT SS
nsy-1(ag3) OP50
nsy-1(ag3) SS
G
WT
tir-1(qd4)
nsy-1(ag3)
200µm
Relative worm length
****
****
n=77
n=90
n=90
WT
nsy-1(ag3)
tir-1(qd4)

Figure 4

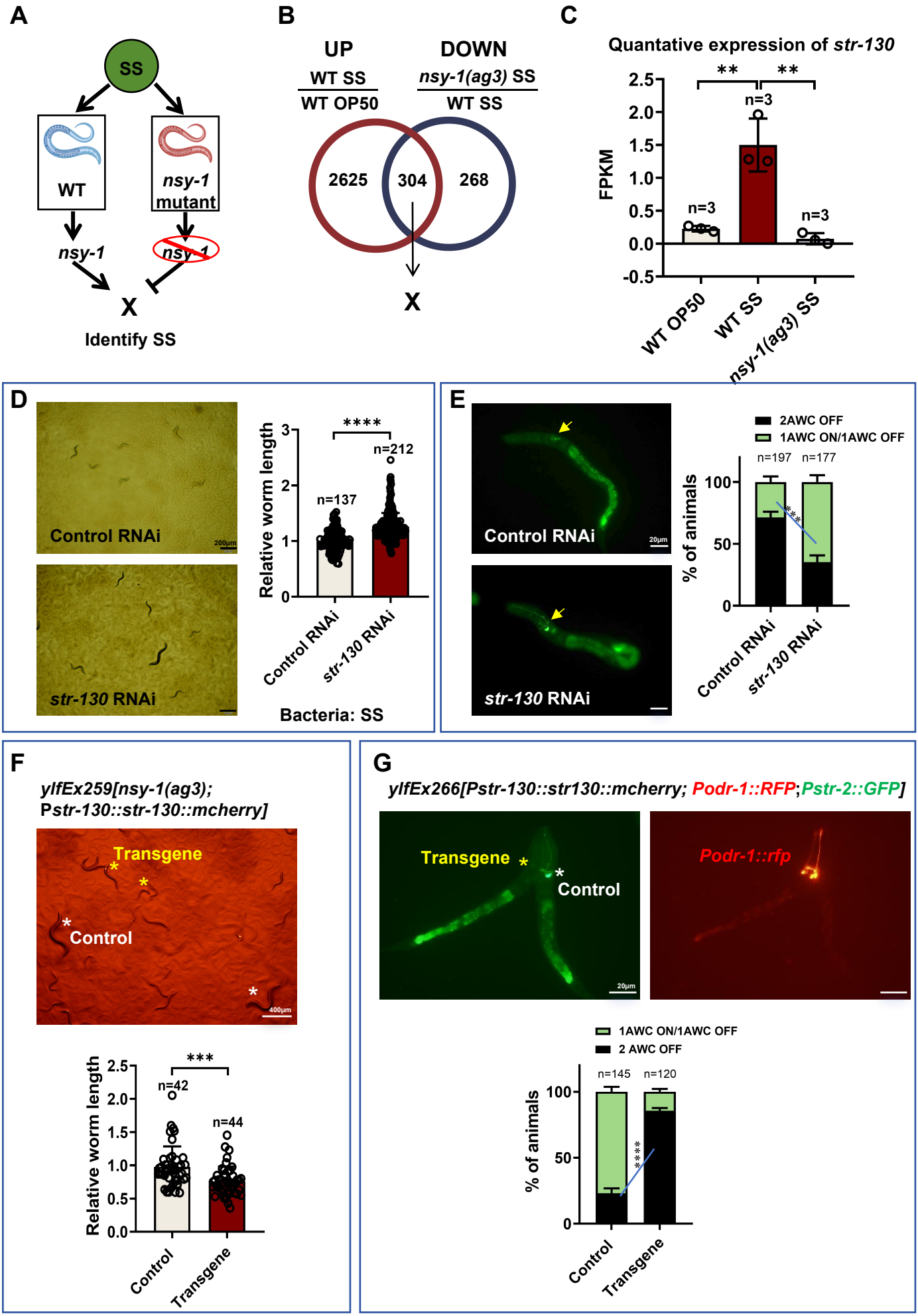
A
SS
WT
nsy-1 mutant
nsy-1
nsy-1
X
Identify SS
B
UP
WT SS
WT OP50
DOWN
nsy-1(ag3) SS
WT SS
2625
304
268
X
C
Quantative expression of str-130
FPKM
n=3
n=3
n=3
WT OP50
WT SS
nsy-1(ag3) SS
D
Control RNAi
str-130 RNAi
Relative worm length
n=137
n=212
Control RNAi
str-130 RNAi
Bacteria: SS
E
Control RNAi
str-130 RNAi
2AWC OFF
1AWC ON/1AWC OFF
n=197
n=177
% of animals
Control RNAi
str-130 RNAi
F
ylfEx259[nsy-1(ag3); Pstr-130::str-130::mcherry]
Transgene
Control
Relative worm length
n=42
n=44
Control
Transgene
G
ylfEx266[Pstr-130::str130::mcherry; Podr-1::RFP;Pstr-2::GFP]
Transgene
Control
Podr-1::rfp
1AWC ON/1AWC OFF
2 AWC OFF
n=145
n=120
% of animals
Control
Transgene

Figure 5

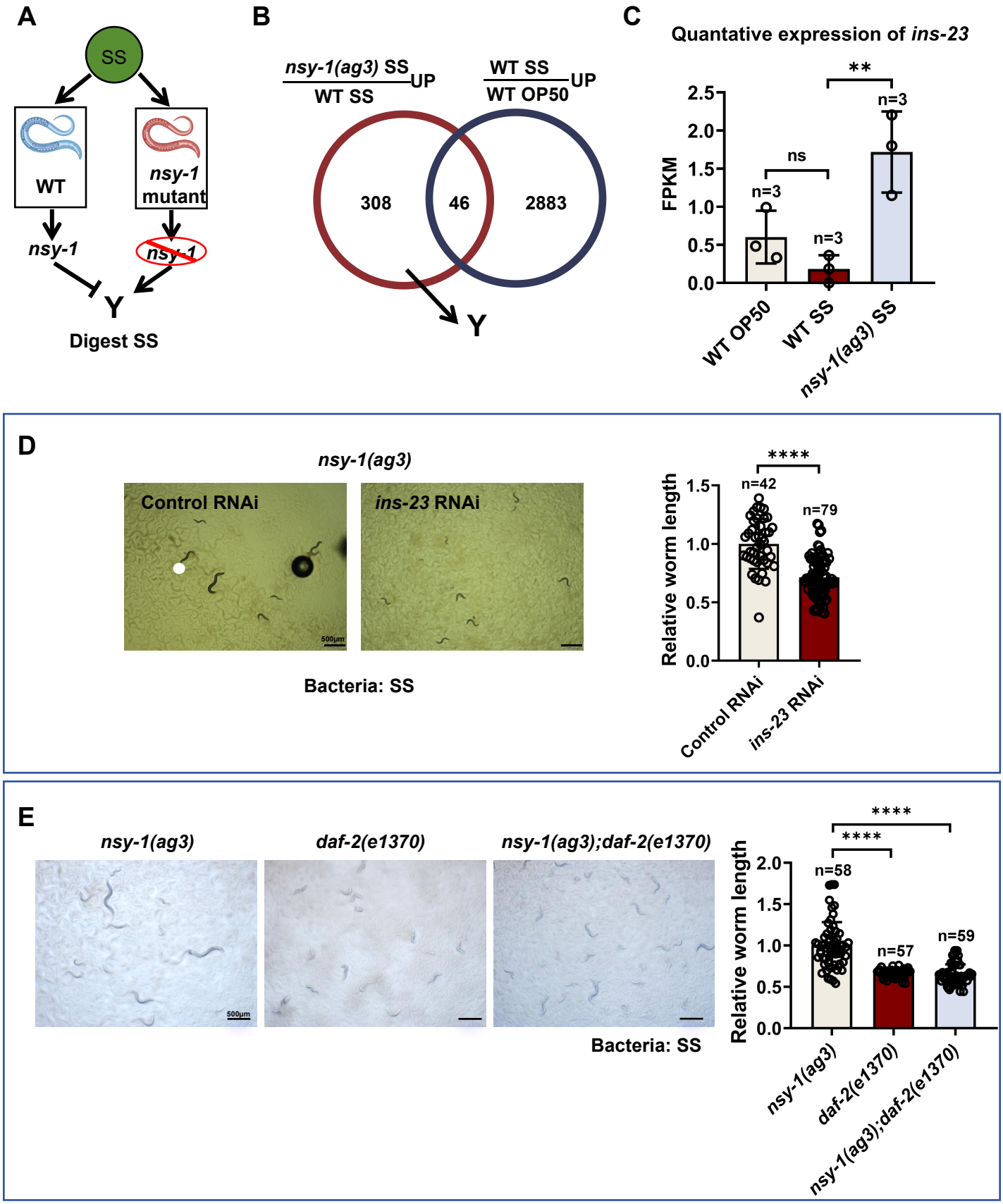
A
SS
WT
nsy-1 mutant
nsy-1
nsy-1
Y
Digest SS
B
nsy-1(ag3) SS / WT SS UP
WT SS / WT OP50 UP
308
46
2883
Y
C
Quantative expression of ins-23
FPKM
2.5
2.0
1.5
1.0
0.5
0.0
**
ns
n=3
n=3
n=3
WT OP50
WT SS
nsy-1(ag3) SS
D
nsy-1(ag3)
Control RNAi
ins-23 RNAi
500μm
Bacteria: SS
Relative worm length
1.5
1.0
0.5
0.0
****
n=42
n=79
Control RNAi
ins-23 RNAi
E
nsy-1(ag3)
daf-2(e1370)
nsy-1(ag3);daf-2(e1370)
500μm
Bacteria: SS
Relative worm length
2.0
1.5
1.0
0.5
0.0
****
****
n=58
n=57
n=59
nsy-1(ag3)
daf-2(e1370)
nsy-1(ag3);daf-2(e1370)

Figure 6

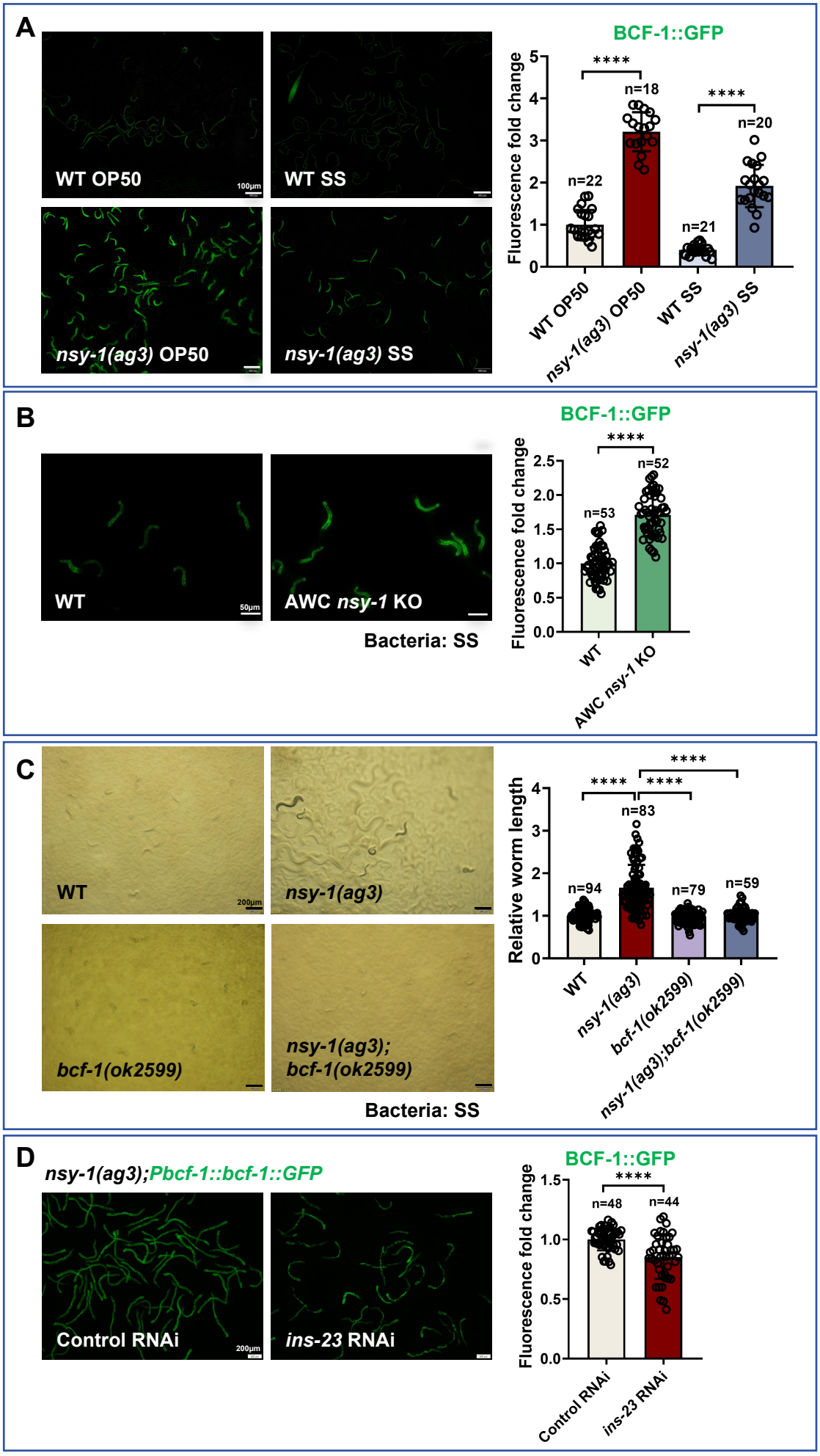
A
WT OP50
100µm
WT SS
nsy-1(ag3) OP50
nsy-1(ag3) SS
BCF-1::GFP
Fluorescence fold change
****
n=22
n=18
n=21
n=20
WT OP50
nsy-1(ag3) OP50
WT SS
nsy-1(ag3) SS
B
WT
50µm
AWC nsy-1 KO
Bacteria: SS
BCF-1::GFP
Fluorescence fold change
****
n=53
n=52
WT
AWC nsy-1 KO
C
WT
200µm
nsy-1(ag3)
bcf-1(ok2599)
nsy-1(ag3);
bcf-1(ok2599)
Bacteria: SS
Relative worm length
****
n=94
n=83
n=79
n=59
WT
nsy-1(ag3)
bcf-1(ok2599)
nsy-1(ag3);bcf-1(ok2599)
D
nsy-1(ag3);Pbcf-1::bcf-1::GFP
Control RNAi
200µm
ins-23 RNAi
BCF-1::GFP
Fluorescence fold change
****
n=48
n=44
Control RNAi
ins-23 RNAi

Figure 7

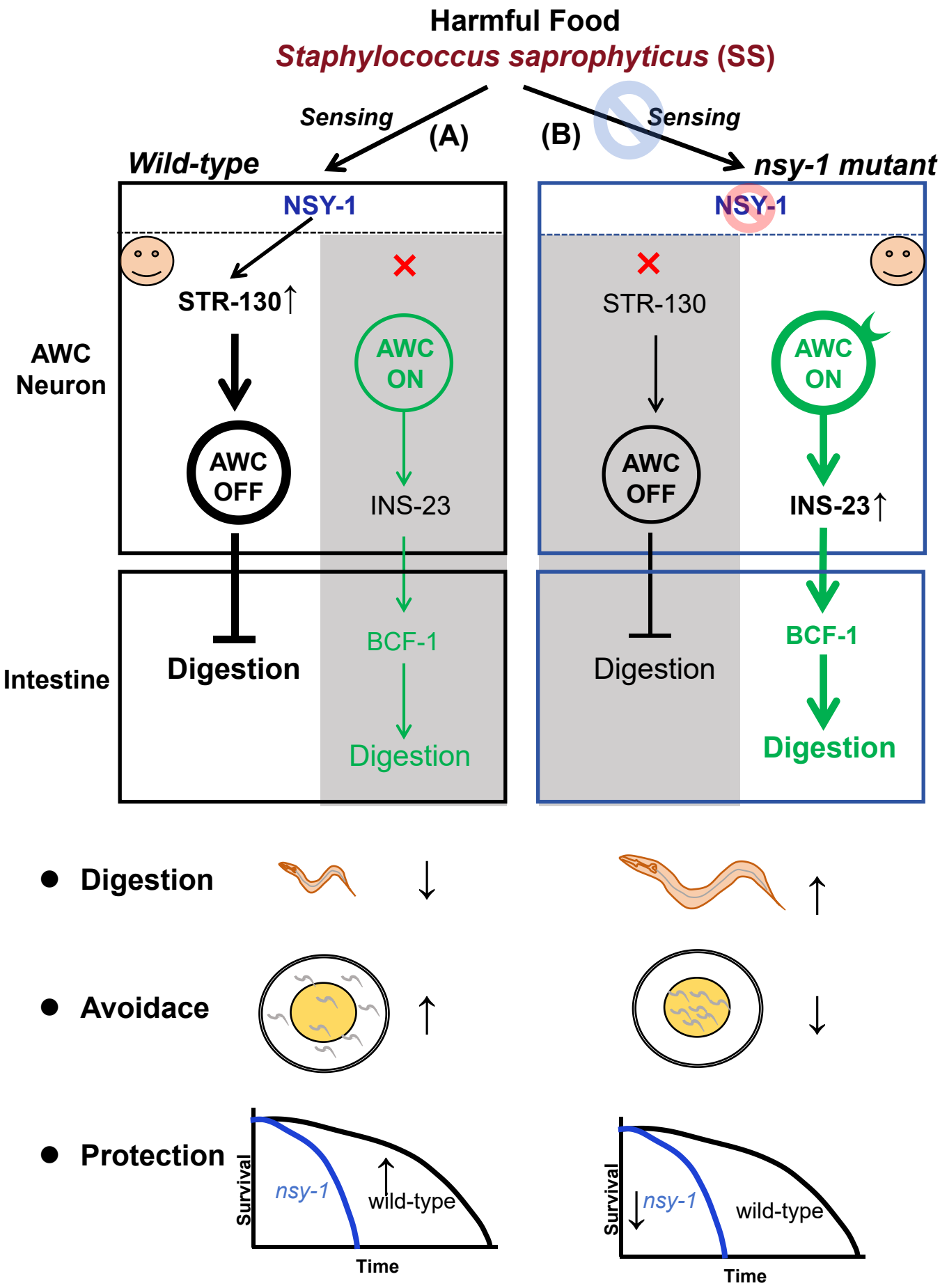
Harmful Food
Staphylococcus saprophyticus (SS)
Sensing
(A)
(B)
Sensing
Wild-type
nsy-1 mutant
NSY-1
NSY-1
STR-130↑
STR-130
AWC Neuron
AWC ON
AWC OFF
INS-23
AWC ON
AWC OFF
INS-23↑
Intestine
Digestion
BCF-1
Digestion
Digestion
BCF-1
Digestion
Digestion
Avoidace
Protection
Survival
nsy-1
wild-type
Time
Survival
nsy-1
wild-type
Time